Modification of Biodistribution and Brain Uptake of Copper Bis(thiosemicarbazonato) Complexes by the Incorporation of Amine and Polyamine Functional Groups

Brett M. Paterson,[†,‡,§] Carleen Cullinane,[⊥,∥] Peter J. Crouch,[¶,∇,#] Anthony R. White,[¶,○] Kevin J. Barnham,[‡,∇,#] Peter D. Roselt,[∥] Wayne Noonan,[∥] David Binns,[∥] Rodney J. Hicks,[⊥,∥] and Paul S. Donnelly*,[†,‡]

[†]School of Chemistry, [‡]Bio21 Molecular Science and Biotechnology Institute, [¶]Department of Pathology, [∇]Department of Pharmacology and Therapeutics, [#]Florey Institute of Neuroscience and Mental Health, and [⊥]The Sir Peter MacCallum Department of Oncology, The University of Melbourne, Parkville, Victoria 3010, Australia

[∥]The Centre for Molecular Imaging and Translational Research Laboratory, The Peter MacCallum Cancer Centre, Melbourne, Victoria 3000, Australia

S *Supporting Information*

ABSTRACT: The synthesis of new bis-(thiosemicarbazonato)copper(II) complexes featuring polyamine substituents via selective transamination reactions is presented. Polyamines of different lengths, with different ionizable substituent groups, were used to modify and adjust the hydrophilic/lipophilic balance of the copper complexes. The new analogues were radiolabeled with copper-64 and their lipophilicities estimated using distribution coefficients. The cell uptake of the new polyamine complexes was investigated with preliminary in vitro biological studies using a neuroblastoma cancer cell line. The in vivo biodistribution of three of the new analogues was investigated in vivo in mice using positron-emission tomography imaging, and one of the new complexes was compared to [^{64}Cu]Cu(atsm) in an A431 squamous cell carcinoma xenograft model. Modification of the copper complexes with various amine-containing functional groups alters the biodistribution of the complexes in mice. One complex, with a pendent (*N*,*N*-dimethylamino)ethane functional group, displayed tumor uptake similar to that of [^{64}Cu]Cu(atsm) but higher brain uptake, suggesting that this compound has the potential to be of use in the diagnostic brain imaging of tumors and neurodegenerative diseases.
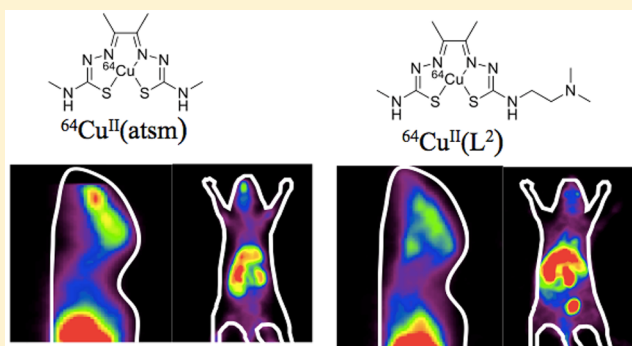
INTRODUCTION

Copper complexes of bis(thiosemicarbazonato) ligands derived from 1,2-diones are of interest as potential diagnostic and therapeutic agents. The ligands can be used to form copper(II) complexes with radioactive isotopes of copper that are stable ($K_a = 10^{18}$), charge-neutral, lipophilic, and capable of crossing cell membranes.[1] The positron-emitting isotopes, ^{60}Cu ($t_{1/2}$ = 24 m), ^{61}Cu ($t_{1/2}$ = 3.33 h), ^{62}Cu ($t_{1/2}$ = 9.75 m), and ^{64}Cu ($t_{1/2}$ = 12.7 h) are of interest in the development of new imaging agents for positron-emission tomography (PET). Copper-64 also has a β^- emission ($E_{\beta^- \text{max}}$ = 0.574 MeV, 40%) that is of potential use in targeted radiotherapy, as does ^{67}Cu ($t_{1/2}$ = 62 h, β^-, 100%, E_{ave} = 0.12 MeV).

The copper complex diacetylbis(4-methyl-3-thiosemicarbazonato)copper(II) [Cu(atsm); Figure 1] has been investigated as a hypoxia imaging agent in tumors and myocardial ischemia.[2−6] Studies on [^{64}Cu]Cu(atsm) have progressed to a phase II human trial as a PET imaging and therapeutic agent for cervical cancer.[7−10] The hypoxia
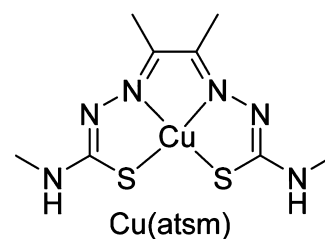

Figure 1. Copper complex Cu(atsm).

selectivity of Cu(atsm) is related to the Cu$^{II/I}$ reduction potential, which leads to selective reduction of the metal ion and subsequent trapping of the radioactivity in certain cells.[3,5,11,12] The high lipophilicity of Cu(atsm) results in high nonspecific cell uptake and liver uptake. The nonspecific
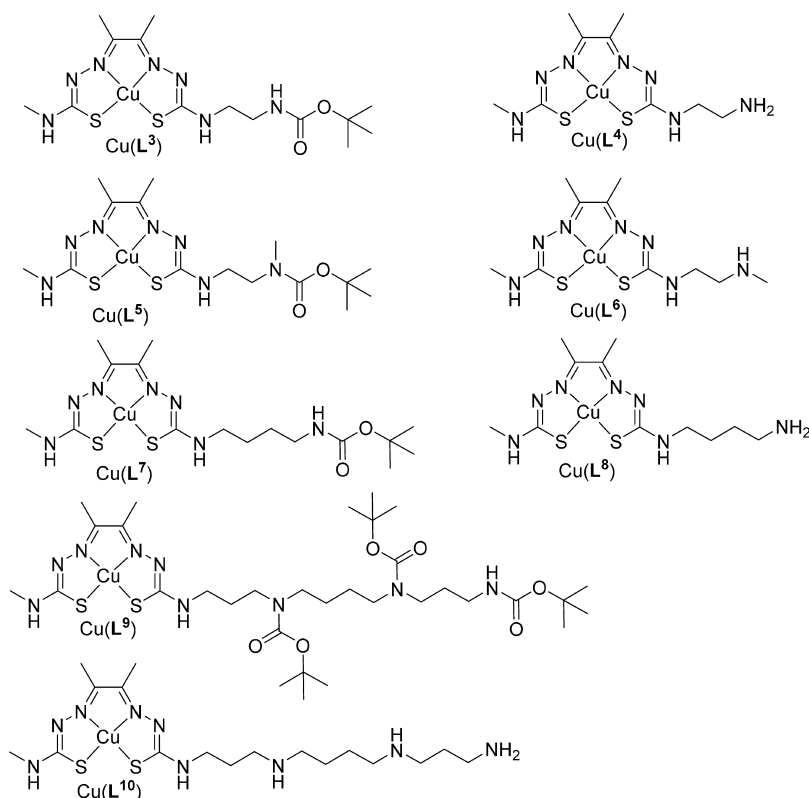
Figure 2. Structures of Cu(L$^{3-10}$).

uptake can compromise the image quality, and the high liver uptake results in dose-limiting radiotoxicity to the liver for therapeutic applications.[13]

The ability of Cu(atsm) to cross the blood–brain barrier has led to radiolabeled [^{62}Cu]Cu(atsm) being investigated as a probe for the redox status of the brain in mitochondrial disease, Parkinson's disease, and amyotrophic lateral sclerosis (ALS).[14−16] In addition to radiopharmaceutical applications, nonradioactive Cu(atsm) has been investigated as a potential therapeutic agent for Parkinson's disease and ALS.[17−23] The therapeutic potential for Cu(atsm) in both ALS and Parkinson's disease is currently being investigated in two human clinical trials.

The biodistribution, cellular accumulation, and metabolism of bis(thiosemicarbazonato)copper(II) [Cu(btsc)] complexes is dependent on their lipophilicity and their Cu$^{II/I}$ reduction potentials.[24,25] The lipophilicity of Cu(btsc) complexes can be altered by changing the nature of both the substituent on the π-conjugated backbone and the terminal (N^4) amine of the ligand.[24,26] In general, changing the aliphatic substituents on the N^4 amine does not affect the redox potential significantly (±0.05 V), especially compared to the changes that can occur as a result of changes in the substituents on the diimine backbone (±0.2 V).[5] Hydrophilic analogues of Cu(atsm) have been identified as potential targets for new hypoxia-selective copper radiopharmaceuticals to reduce the level of liver and kidney uptake.[27−30]

We have prepared a series of new bis(thiosemicarbazones) with amine and polyamine functional groups with the goal of producing complexes with biodistribution profiles different from those of Cu(atsm). The biogenic polyamines butane-1,4-diamine (putrescine), *N*-(3-aminopropyl)butane-1,4-diamine (spermidine), and *N,N′*-bis(3-aminopropyl)butane-1,4-dia-

mine (spermine) are ubiquitous in nearly every prokaryotic and eukaryotic cell type and have been used to increase the blood–brain barrier permeability of therapeutic peptides and proteins.[31−33] In aqueous solution at pH 7.4, the polyamines are fully protonated, giving them considerable water solubility. Polyamine side chains have been shown to enhance the cellular uptake and specificity of anticancer pharmaceuticals and imaging agents by a combination of utilization of polyamine transport systems and the ability of polyamines and alkylated amine functional groups to modify the hydrophobic–lipophilic character as well as overall charge and solvation.[34−43]

The synthesis of new Cu(btsc) complexes featuring polyamine substituents via selective transamination reactions is presented. Polyamines of different lengths, numbers of charged groups, and substituent groups were used to modify and adjust the hydrophilic/lipophilic balance of the copper complexes. The new analogues were radiolabeled with ^{64}Cu, and their distribution coefficients were determined. The cell uptake of the new polyamine complexes was investigated with preliminary in vitro biological studies using a neuroblastoma cancer cell line because hypoxia is a strong independent risk predictor in neuroblastoma patients.[44] We also examined the in vivo biodistribution of three of the new analogues using in vivo small-animal PET imaging and selected one complex for evaluation in an A431 squamous cell carcinoma xenograft model.

■ RESULTS AND DISCUSSION

Synthesis of Bis(thiosemicarbazone)−Polyamines and Their Copper Complexes. Selective transamination reactions of the nonsymmetric molecule H$_2$L^1 with nucleophilic amines resulting in the selective displacement of dimethylamine from the dimethyl substituent have proven to

Scheme 1. Synthesis of H$_2$L^2 and Cu(L^2)^a
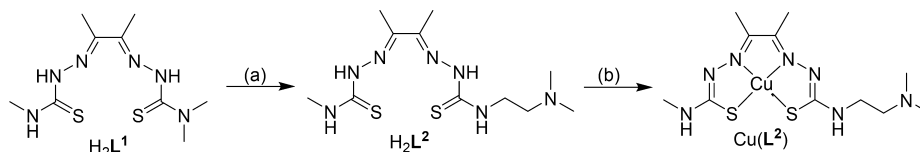
^{a}(a) *N,N*-Dimethylethylenediamine (1.3 equiv), acetonitrile, reflux, 6.5 h, 74%. (b) Cu(CH$_3$CO$_2$)$_2$·H$_2$O (1 equiv), acetonitrile, reflux, 1.5 h, 75%.

be a reliable method to prepare substituted bis-(thiosemicarbazone) (Figure 2).[29,45−48] The incoming amine reacts with the electrophilic thiocarbonyl carbon atom of N^4,N^4-dimethylthiosemicarbazone substituents with preference toward the N^4-monosubstituted moiety, which is capable of undergoing tautomerization. A family of bis-(thiosemicarbazones) complexes were prepared where short-chain polyamines, 1,2-diaminoethane, *N,N*-dimethylethylene-diamine, and *N*-methylethylenediamine, as well as the biogenic polyamines putrescine and spermine, were appended to the ligand framework. The reaction of *N,N*-dimethylethylenedi-amine with H$_2$L^1 allowed the isolation of H$_2$L^2 in high yield. The copper complex was prepared by reacting H$_2$L^2 with copper acetate monohydrate, which leads to double deproto-nation of the ligand and the formation of charge-neutral Cu(L^2) (Scheme 1).

The reactions with polyamines that contain more than one nucleophilic amine required selective protection, with *N-tert*-butoxycarbonyl (*t*-Boc) groups (Figure 2). The syntheses of [H$_3$L^4][CF$_3$CO$_2$] and [Cu(H$_2$L^4)][CF$_3$CO$_2$]$_2$ were described previously (Figure 2) but are included.[45] Both the primary and secondary amines of *N*-methylethylenediamine are sufficiently nucleophilic to complicate a transamination reaction. To prevent the secondary amine from reacting, it was protected with a *t*-Boc group. The primary amine was first protected using a trifluoroacetamide group.[49] Ethyl trifluoroacetate reacts preferentially with the primary amine under controlled conditions. The *t*-Boc group was added to the secondary amine before trifluoroacetamide was removed in a basic solution. The resulting product was subjected to trans-amination to give the product H$_2$L^5, and the copper complex Cu(L^5) was prepared by the addition of copper acetate monohydrate (Figure 2).

The room temperature ^{1}H and ^{13}C{^{1}H} NMR spectra of H$_2$L^5 contain broadened signals and signals that have been divided in two. These signals correspond to proton and carbon environments near the carbamate bond. The signals due to the bis(thiosemicarbazone) groups were much sharper in compar-ison. In the ^{13}C{^{1}H} NMR spectrum, the signals are split into two peaks for the methylene (δ = 41.7, 42.5 and 46.6, 47.3), carbonyl (δ = 154.7, 155.5), *N*-methyl (δ = 34.0, 34.4), and quaternary (δ = 78.3, 78.6) carbon atoms (Figure S1). A likely explanation is that electron delocalization results in partial double-bond character for the carbamate group and hindered rotation about the C(carbonyl)−N bond (Figure S2). The partial double-bond character renders the carbamate group planar, with it existing in either the s-cis or s-trans rotamer. Hindered rotation about secondary amide peptide bonds and carbamates is known.[50−53] At room temperature, both isomers are observed in the NMR spectrum as a result of slow interconversion between the two forms relative to the NMR time scale. Coalescence of the isomeric signals was observed as the temperature was increased. At 70 °C, a single broad peak

was observed for the methylene (δ = 42.0 and 46.8) carbonyl (δ = 155.0), *N*-methyl (δ = 34.0), and quaternary (δ = 78.3) carbon atoms, which indicates that the rate of interconversion was now faster than the time scale of the NMR experiment. The electron-donating *N*-methyl group of the carbamate on H$_2$L^5 may be stabilizing the C(carbonyl)−N double-bond form, thus increasing the barrier to C(carbonyl)−N bond rotation.[54,55] In contrast, isomerization was not observed in the room temperature NMR spectra of H$_2$L^3 because the partial double bond is less stabilized, leading to faster interconversion between the s-cis and s-trans isomers.

The *t*-Boc protecting group of H$_2$L^5 and Cu(L^5) was removed with trifluoroacetic acid to give [H$_3$L^6][CF$_3$CO$_2$] and [Cu(HL^6)][CF$_3$CO$_2$]·0.8CF$_3$CO$_2$H, respectively. The electro-spray ionization mass spectrometry (ESI-MS) spectrum of [Cu(HL^6)][CF$_3$CO$_2$]·0.8CF$_3$CO$_2$H (m/z 365.05; 100%) corresponded to that of [Cu(HL^6)]$^+$, and reverse-phase high-performance liquid chromatography (RP-HPLC; R_T = 7.424 min) indicated successful deprotection, while the microanalysis suggested the presence of trifluoroacetate as the counterion.

One of the primary amines of the polyamine putrescine was protected with *t*-Boc using a literature procedure.[56] Trans-amination of H$_2$L^1 with *t*-Boc-protected polyamine *tert*-butyl 4-aminobutylcarbamate produced H$_2$L^7 in high yield (Figure 2). To ensure a selective transamination reaction with one of the primary amine groups of spermine, one of the primary amines and both secondary amines were protected using *t*-Boc. The tri-*t*-Boc spermine compound was prepared using a literature procedure.[57] The transamination reaction between H$_2$L^1 and (N^1,N^4,N^9-tri-*tert*-butoxycarbonyl)-*N,N'*-bis(3-aminopropyl)-butane-1,4-diamine gave H$_2$L^9 in good yield following silica chromatography. Signals in the ^{1}H and ^{13}C{^{1}H} NMR spectra were broad when obtained at room temperature, possibly because of cis/trans isomerism of the three carbamate bonds. Increasing the temperature to 70 °C sharpened some of the signals, allowing the spectra to be more easily assigned with two-dimensional NMR spectroscopy. The ESI-MS spectrum gave a peak at m/z 732.43 (100%), corresponding to [H$_2$L^9 + H$^+$], and the RP-HPLC had a single peak (R_T = 18.16 min). The copper complex Cu(L^9) (m/z 793.34; 100%; R_T = 17.40 min) was prepared with the addition of copper acetate monohydrate to a solution of H$_2$L^9 in ethanol (Figure 2). Deprotection of H$_2$L^9 and Cu(L^9) with trifluoroacetic acid gave the trications [H$_5$L^{10}][CF$_3$CO$_2$]$_3$ and [Cu(H$_3$L^{10})]-[CF$_3$CO$_2$]$_3$·2H$_2$O (Figure 2), respectively. ESI-MS spectra for [Cu(H$_3$L^{10})][CF$_3$CO$_2$]$_3$·2H$_2$O (m/z 493.18 and 247.10; 100%) corresponded to [Cu(HL^{10})]$^+$ and [Cu(H$_2$L^{10})]$^{2+}$, respectively.

Electrochemical Characterization, Radiolabeling with ^{64}Cu, and Distribution Coefficients. The hypoxia selectivity and biological activity of the Cu(btsc) complexes strongly correlate with the Cu$^{II/I}$ reduction potential. The new complexes Cu(L$^{2−10}$) all retain the methyl substituents on

the diimine-like backbone to ensure that they display $Cu^{II/I}$ couples similar to those of Cu(atsm). The electrochemistry of the new complexes was investigated by cyclic voltammetry. The median potentials ($\overline{E}$) and peak separations ($E_{pa} - E_{pc}$; Table 1) reveal no significant differences between the

Table 1. Median Potentials and Peak Separations of the Cyclic Voltammograms (Scan Rate 0.1 V s^{-1}; Potentials Are Quoted Relative to a SCE)

compound	Cu(atsm)	Cu(L^2)	Cu(L^6)	Cu(L^8)	Cu(L^{10})
Cu^{II}/Cu^{I} $\overline{E}$ (V)	−0.63	−0.65	−0.60	−0.65	−0.63
Cu^{II}/Cu^{I} $E_{pa}-E_{pc}$ (mV)	102	105	104	92	89

complexes. For example, Cu(L^2) has a quasi-reversible reduction with a median potential[58−60] $\overline{E}$ = −0.65 V [vs standard calomel electrode (SCE), where $\overline{E} = (E_{pc} + E_{pa})/2$ and ferrocene/ferrocinium (Fc/Fc$^+$) = 0.54 V] with an anodic-to-cathodic peak separation of 105 mV in N,N-dimethylformamide (DMF) at a glassy carbon working electrode, which was attributed to a Cu$^{II/I}$ reduction process (Figure 3A and Table 1). Deprotection of the complexes with trifluoroacetic acid led to their isolation as aminium salts, and cyclic voltammetry of these protonated cationic salts revealed irreversible reduction waves characteristic of the adsorption of a reduced species to the working electrode (Figure S3A). Neutralization of the protonated cations with triethylamine resulted in the observation of quasi-reversible Cu^{II}/Cu^{I} couples (Figure S3B).

The copper-64 complexes were prepared by the addition of ^{64}Cu (0.02 M HCl, pH 1) to a buffered solution of the ligands (pH ∼7). The complexes were prepared at a specific activity range of 0.74−3.7 GBq mg^{-1} of the ligand. The purities of the complexes were confirmed using HPLC coupled to a radioactivity detector and a comparison with the HPLC traces of the nonradioactive analogues (λ = 280 nm). All of the radiolabeled complexes could be prepared at room temperature in minutes under mild conditions with >90% radiochemical purity without additional purification, making them ideal candidates for in vivo imaging.

The respective retention times of the RP-HPLC traces highlighted the differences in lipophilicity between the complexes and were quantified by obtaining the distribution coefficients (log D at pH 7.4) in phosphate-buffered saline (PBS; Figure 4). Cu(atsm) possessed the highest log D, pH 7.4, value of 1.49 ± 0.08 and a retention time of 10.12 min. Of the new derivatives, the ligand featuring a dimethylamine
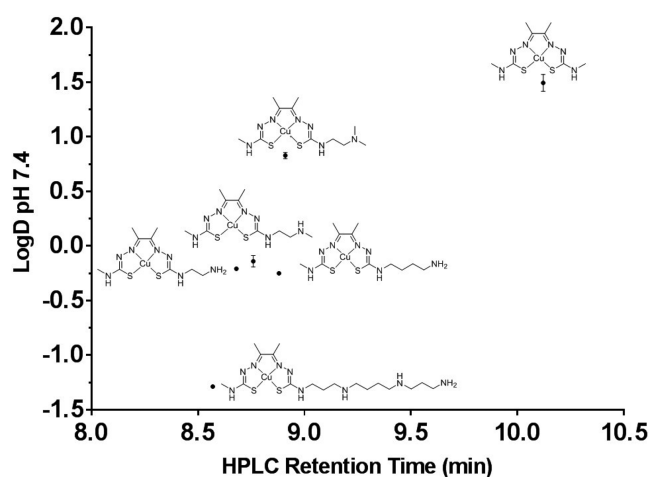
Figure 4. RP-HPLC retention times (R_T) versus the distribution coefficients (log D at pH 7.4) of Cu(atsm) and the new polyamine copper-64 complexes.

substituent, Cu(L^2), was the most lipophilic (0.83 ± 0.03 and 8.91 min) and the spermine derivative the most hydrophilic (−1.29 ± 0.01). The complexes possessing either a single primary amine, Cu(L^4) and Cu(L^8), or a single secondary amine, Cu(L^6), had similar lipophilicities (−0.21 ± 0.02, −0.25 ± 0.01, and −0.14 ± 0.05, respectively).

Cytotoxicity and Cellular Uptake of Bis-(thiosemicarbazonato)copper(II) Complexes. The copper content of SH-SY5Y cells, a neuroblastoma cell line, treated with either Cu(L^2), Cu(L^4), Cu(L^6), Cu(L^8), or Cu(L^{10}) (10 μM, 1 h) was measured by inductively coupled plasma mass spectrometry (ICP-MS; Figure 5a). The highest level of cellular copper was observed in cells treated with the complex Cu(L^2), where a (62 ± 2)-fold increase in the copper levels was detected compared to vehicle-treated controls. This value was greater than the value detected for Cu(atsm) [(47 ± 5)-fold increase]. Significant increases in the copper content (35−37-fold) were observed for the complexes [Cu(H$_2$L^4)]$^{2+}$, [Cu(HL^6)]$^+$, and [Cu(HL^8)]$^+$, which have either a single primary or secondary amine. The complex [Cu(H$_3$L^{10})]$^{3+}$, which has two secondary amines and one primary amine that are likely protonated at biological pH, showed significantly less uptake than the other complexes including unchelated Cu^{2+} (a 3-fold compared to a 5-fold increase in the copper levels).
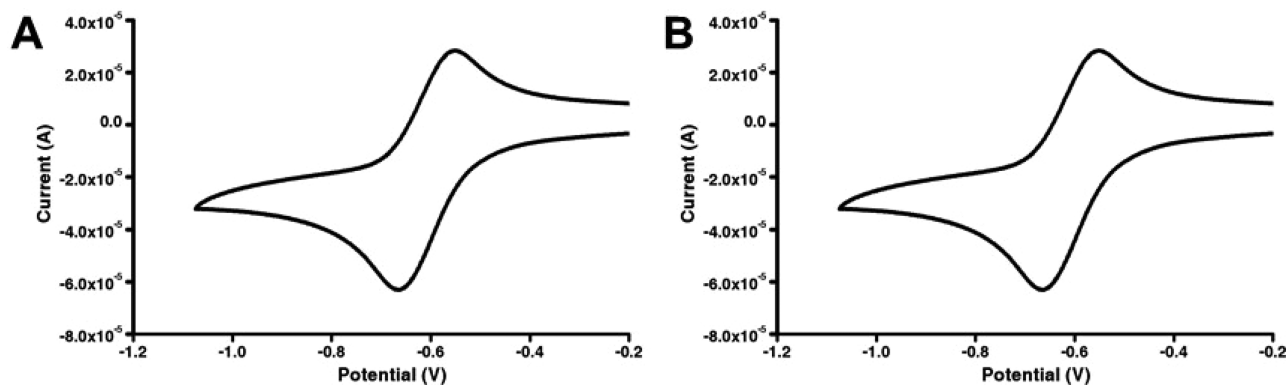
Figure 3. (A) Cyclic voltammogram of Cu(L^2). (B) Cyclic voltammogram of Cu(L^6) in the presence of triethylamine. Scan rate 0.1 V s^{-1}. Potentials are quoted relative to a SCE, where Fc/Fc$^+$ = 0.54 V.
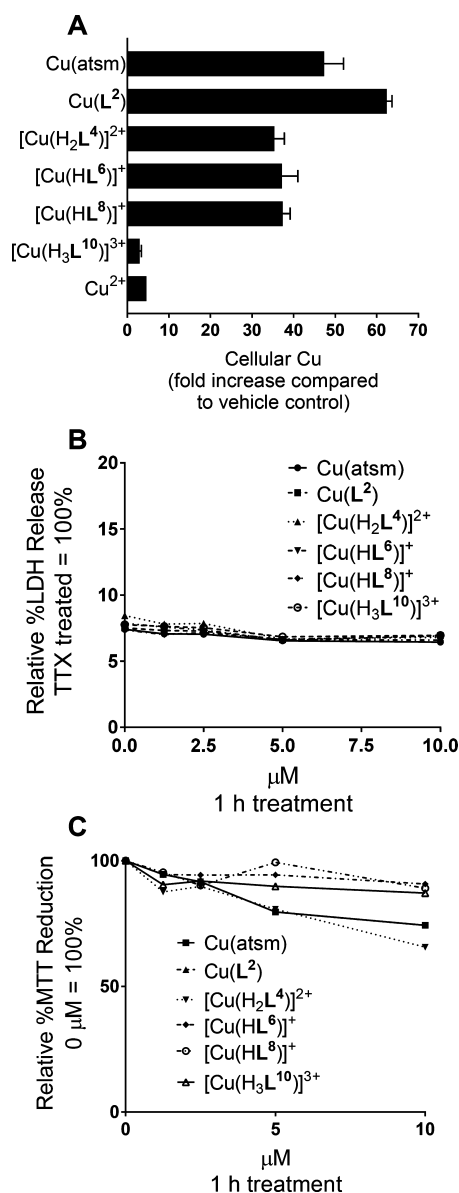
Figure 5. (A) Copper levels in SH-SY5Y cells treated with Cu(btsc) complexes (10 μM) and with CuSO$_4$ (10 μM) for 1 h. The metal levels were measured in washed cell pellets by ICP-MS and calculated as a fold increase compared with the vehicle controls. (B) Dose–response curve for the LDH assay. SH-SY5Y cells were treated with the Cu(btsc) complexes (0, 2.5, 5.0, 7.5, and 10 μM) for 1 h. The LDH levels are presented as the relative % LDH release of Triton X-100-treated total LDH release (100% LDH release). (C) Dose–response curve for the MTT assay. SH-SY5Y cells were treated with the Cu(btsc) complexes (0, 2.5, 5.0, 7.5, and 10 μM) for 1 h. The MTT levels are presented as the relative % MTT reduction of vehicle-treated cells (100% MTT reduction).

The lactate dehydrogenase (LDH) assay measures membrane integrity and can be used to assess the cytotoxicity.[61,62] The neuroblastoma SH-SY5Y cells were treated with Cu(btsc) complexes at concentrations ranging from 1–10 μM for 1 h. The dose–response curve for the release of LDH, following treatment with the copper complexes, indicates that there is ~5% cell death, but there are no dose-dependent changes over the concentration range tested (Figure 5b). The cell membrane integrity is therefore maintained upon exposure to the Cu(btsc) complexes at the concentrations investigated.

The 3-(4,5-dimethylthiazol-2-yl)-2,5-diphenyltetrazolium bromide (MTT) assay measures the inhibition of reductase enzymes and therefore the cell viability upon exposure to chemical compounds.[63] The dose–response curve for the MTT assay indicates that the complexes Cu(atsm) and Cu(L^2) were the only complexes that inhibited intracellular reductase activity in a dose-dependent manner (Figure 5c), and up to concentrations of 10 μM, the inhibition of the reductase activity was relatively small. The complexes Cu(L^2) and Cu(atsm), which have the highest cellular copper uptake, exhibit a modest dose-dependent inhibition of intracellular reductase activity and are the most lipophilic compounds in the series tested.

The addition of polyamines to the ligand framework of the Cu(btsc) complexes allows for subtle control of the lipophilicity but retains the electrochemical features [a Cu$^{II/I}$ reduction potential $E^{\circ\prime} \sim -0.63$ V (vs SCE)], which are thought to be important to the hypoxia selectivity and biological activity of Cu(atsm). The addition of a dimethylamine group in complex Cu(L^2) increased the amount of copper transported into SH-SY5Y cells compared to Cu(atsm). Although the addition of either a primary or secondary amine group (complexes [Cu(H$_2$L^4)]$^{2+}$, [Cu(HL^4)]$^+$, and [Cu(HL^8)]$^+$) reduced the cellular copper uptake compared to Cu(atsm), these values (35–37-fold increase) were consistent and still significantly greater than those obtained following treatment with unchelated Cu^{2+}. The addition of two secondary amines and a primary amine in the case of [Cu(H$_3$L^{10})]$^{3+}$ saw a significant decrease in the uptake of copper compared to Cu(atsm). Bis(thiosemicarbaonato)-copper(II) complexes are notorious for being poorly soluble in water, but [Cu(H$_3$L^{10})]$^{3+}$, the most hydrophilic complex in this series, is soluble in water at pH 7.4 at millimolar concentrations.

Small-Animal PET Imaging. Three of the new copper-64 complexes, [^{64}Cu]Cu(L^2), [^{64}Cu]Cu(L^6), and [^{64}Cu]Cu(L^8), were selected for preliminary in vivo biodistribution studies using small-animal microPET imaging and compared to Cu(atsm). Mice (Balb/c) were administered radioactive copper complexes (15–20 MBq) via intravenous tail vein injection and imaged 5 min postinjection (Figure 6). Qualitative analysis of the images reveals that the biodistribution at 5 min postinjection of each of the new compounds is dramatically different from that of [^{64}Cu]Cu(atsm)], which is rapidly taken up in the liver (Figure 6). The images are also different from the PET images obtained following administration of "free" nonchelated copper-64.[64,65] The difference in the microPET images of [^{64}Cu]Cu(L^2), [^{64}Cu]Cu(L^6), and [^{64}Cu]Cu(L^8) compared to [^{64}Cu]Cu(atsm) and nonchelated ^{64}Cu suggests that the complexes are sufficiently stable in vivo to provide imaging agents with a different biodistribution at early time points (5 min postinjection). All three new complexes appear to have increased uptake in the kidney and bladder compared to [^{64}Cu]Cu(atsm), suggesting a shift from predominant hepatobiliary to a combination of renal and hepatobiliary clearance. The complexes with a secondary amine, [^{64}Cu]Cu(L^6), and a primary amine functional group, [^{64}Cu]Cu(L^8), showed little to no radioactivity in the brain. The complex with a pendent secondary amine, [^{64}Cu]Cu(L^2), had a relatively high level of uptake in the brain and did not have the prominent high degree of uptake in the olfactory bulb that is evident in the images acquired following the administration of [^{64}Cu]Cu(atsm).[66,67]
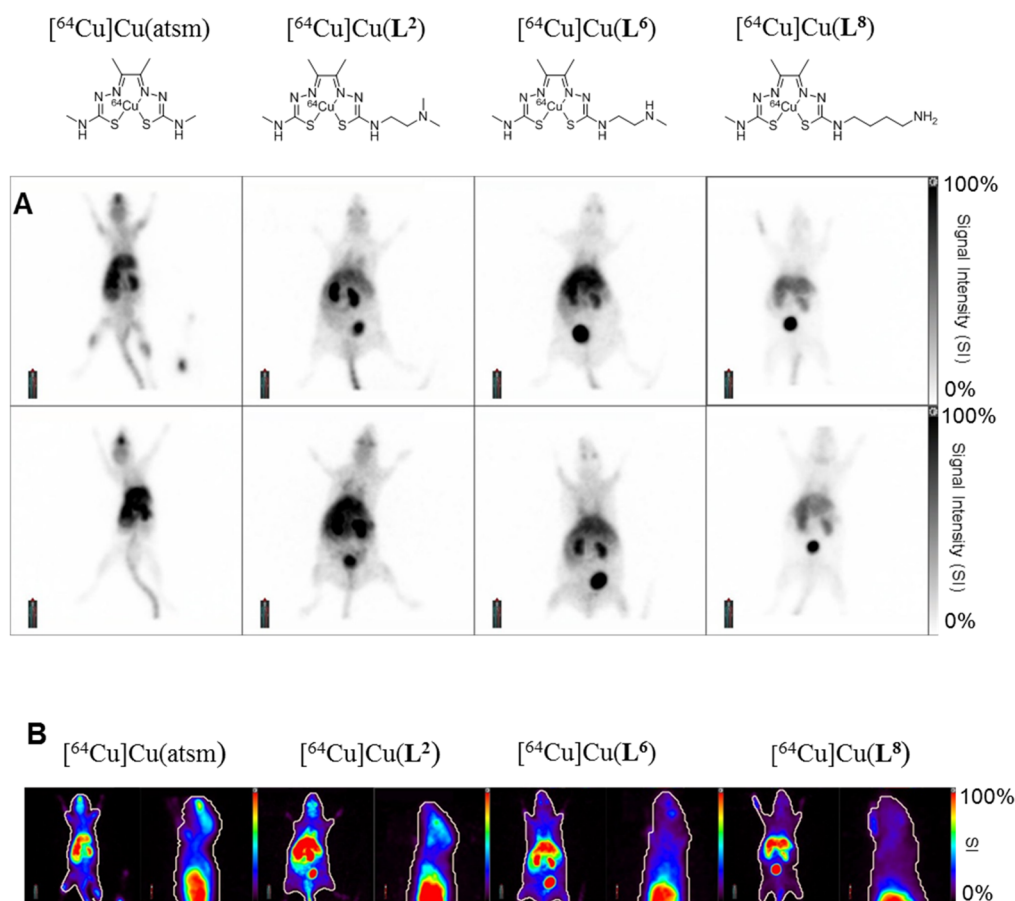
Figure 6. (A) Small-animal microPET images (maximum-intensity projection) of two BALB/c mice 5 min after a single intravenous administration of 15−20 MBq of $[^{64}Cu]Cu(atsm)$, $[^{64}Cu]Cu(L^2)$, $[^{64}Cu]Cu(L^6)$, and $[^{64}Cu]Cu(L^8)$. The animals were placed on the bed of a Philips Mosaic small-animal PET scanner 5 min postinjection and imaged over 10 min. (B) Representative false color images: close-up of the brain region (sagittal plane) and maximum-intensity projection.

Tumor Uptake and Biodistribution in a A431 Tumor Model. The hypoxia-selective retention of radioactivity from $[^{62}Cu]Cu(atsm)$ in an ex vivo rat heart model of ischemia stimulated much interest in the potential to use radiolabeled versions of Cu(atsm) as hypoxia imaging agents.[3] The hypoxia-selective retention of radioactivity following the treatment of EMT6 cells with $[^{64}Cu]Cu(atsm)$ has been demonstrated in vitro.[68] The tumor uptake of copper-64 following injection of $[^{64}Cu]Cu(atsm)$ to BALB/c mice bearing EMT6 tumors was $4.17 \pm 1.03\%$IA/g (%IA/g = injected activity per gram of tissue) at 40 min postinjection, and the retention was attributed to hypoxia.[68] Injection of either $[^{64}Cu]Cu(atsm)$ or $[^{64}Cu]Cu(CH_3CO_2)_2$ in mice bearing CaNT or EMT6 tumors resulted in similar degrees of copper-64 retention in the representative tumors at 2 and 16 h postinjection, and the areas of uptake correlated with the areas of hypoxia identified by immunohistochemistry. However, the copper uptake following the administration of either $[^{64}Cu]Cu(atsm)$ or $[^{64}Cu]Cu(CH_3CO_2)_2$ at earlier time points (15 min and 2 h postinjection) did not correlate to areas of hypoxia in this model.[69] Despite the similarities between the biodistribution of $[^{64}Cu]Cu(atsm)$ and $[^{64}Cu]Cu(CH_3CO_2)_2$ at later time points, radioactive copper complexes of bis-(thiosemicarbazonato) ligands do not behave like unchelated copper in the early phase of biodistribution. There is a dramatic difference in the brain uptake of $[^{64}Cu]Cu(atsm)$ and $[^{64}Cu]Cu(CH_3CO_2)_2$.[66,67]

The difference in the biodistribution of $[^{64}Cu]Cu(L^2)$ and $[^{64}Cu]Cu(atsm)$ revealed by PET imaging at 5 min post-injection coupled with the relatively high brain uptake displayed by $[^{64}Cu]Cu(L^2)$ encouraged us to select this compound for evaluation in a tumor model. The new tracer, $[^{64}Cu]Cu(L^2)$, was compared with $[^{64}Cu]Cu(atsm)$ in an A431 squamous cell carcinoma xenograft model that leads to intratumoral hypoxia.[70] Mice were administered with either $[^{64}Cu]Cu(L^2)$ or $[^{64}Cu]Cu(atsm)$ via intravenous tail vein injection (10−15 MBq) and imaged with a small-animal PET scanner at 1, 3, and 22 after tracer injection. The microPET imaging data reveal that at each time point the standardized uptake values (SUVs) in the tumor for $[^{64}Cu]Cu(L^2)$ and $[^{64}Cu]Cu(atsm)$ are not significantly different ($p > 0.08$; Table 2).

Following the final scan, the mice were culled and tissues excised for an ex vivo biodistribution analysis (Table 3). The administration of $[^{64}Cu]Cu(atsm)$ and $[^{64}Cu]Cu(L^2)$ leads to

Table 2. Tumor SUV Data (SUV $\pm$ Standard Error; $n = 3$) As Determined by Small-Animal PET Imaging

time (h)	$[^{64}Cu]Cu(atsm)$	$[^{64}Cu]Cu(L^2)$
1	0.61 ± 0.05	0.79 ± 0.08
3	0.70 ± 0.02	0.81 ± 0.06
22	0.78 ± 0.05	0.99 ± 0.08

Table 3. Biodistribution (%IA/g ± Standard Error; $n = 3$) at 23 h Postinjection

	[64Cu]Cu(atsm)	[64Cu]Cu(L²)
blood	2.34 ± 0.28	2.98 ± 0.56
lungs	6.79 ± 0.44	15.53 ± 1.47
heart	3.58 ± 0.42	5.42 ± 0.35
liver	14.27 ± 1.96	16.59 ± 3.08
kidneys	5.98 ± 0.55	8.97 ± 0.45
muscle	0.74 ± 0.07	1.42 ± 0.05
spleen	5.04 ± 0.22	4.62 ± 0.77
brain	2.43 ± 0.31	4.41 ± 0.23
eyes	1.06 ± 0.14	1.97 ± 0.60
tumor	2.59 ± 0.20	3.35 ± 0.20

tumor uptakes of 2.59 ± 0.20%IA/g and 3.35 ± 0.20%IA/g, respectively, 23 h after injection ($p < 0.06$). The degree of uptake observed 16 h postinjection of [64Cu]Cu(atsm) to CBA mice bearing CaNT tumors was 1.32 ± 0.09%IA/g.[69] The A431 squamous cell carcinoma xenograft model used in this study has been previously shown to lead to intratumoral hypoxia, but a limitation of this present study is that, in this instance, the tumors were not confirmed as hypoxic using immunohistochemistry.[70] Considering that injection of either [64Cu]Cu(atsm) or [64Cu]Cu(CH₃CO₂)₂ in mice bearing CaNT or EMT6 tumors resulted in similar degrees of copper-64 retention at 16 h postinjection, it would be pertinent to have included [64Cu]Cu(CH₃CO₂)₂ in the present study and to investigate the in vivo stability of the two complexes.[69] It is possible that the uptake of copper-64 in tumors at 16 h postinjection actually reflects endogenous copper metabolic pathways involving specific chaperone and transport proteins as well as cuproenzymes rather than specific uptake mediated by the injected complex.[71−73] Significant differences were found between the biodistribution of the two tracers in the lungs, kidneys, heart, muscle, and brain ($p < 0.05$) at 23 h postinjection. The ability of Cu(atsm) to cross the blood−brain barrier has led to radiolabeled [62Cu]Cu(atsm) being used to distinguish the tumor grade in human glioma patients,[74] and treatment with [64Cu]Cu(atsm) was investigated recently as a therapeutic option in a mouse model of glioblastoma.[75] Brain imaging with [62Cu]Cu(atsm) has also been used to probe the redox status in human patients with mitochondrial disease,[14] Parkinson's disease,[15] and ALS.[16] The administration of [64Cu]Cu(L²) leads to more radioactivity in the brain, 4.41 ± 0.23%ID/g, compared to that of [64Cu]Cu-(atsm), 2.43 ± 0.31%ID/g, ($p < 0.01$), suggesting that this new variant could be of interest as a brain imaging agent. The addition of the same functional group to copper complexes of functionalized pyridylthiosemicarbazone ligands also improved brain uptake.[76]

CONCLUSION

A range of new Cu(btsc) complexes with amine and polyamine functional groups have been prepared using a selective transamination reaction. The addition of the amine functional groups reduces the lipophilicity of these derivatives of Cu(atsm) but does not significantly alter the Cu^{II/I} reduction potential that is thought to be central to the biological activity of this type of complex. With the exception of the complex that incorporates a spermine functional group, [Cu(H₃L¹⁰)]³⁺, the complexes were all capable of dramatically increasing the intracellular copper content of neuroblastoma SH-SY5Y cells,

suggesting that they retain the ability of Cu(atsm) to cross cell membranes, which is also thought to be crucial to the biological activity of this family of complexes. The biodistribution in mice of three of the new complexes, [64Cu]Cu-(L²), [64Cu]Cu(L⁶), and [64Cu]Cu(L⁸), was investigated using microPET imaging and revealed that each of these less lipophilic derivatives of [64Cu]Cu(atsm) has a different early biodistribution compared to [64Cu]Cu(atsm). The difference in the biodistribution of [64Cu]Cu(L²) and [64Cu]Cu(atsm) revealed by a preliminary PET imaging study and the relatively high brain uptake encouraged us to evaluate this compound in an A431 tumor model. In this model, the administration of [64Cu]Cu(L²) leads to tumor uptake (3.35 ± 0.20%IA/g) 23 h postinjection similar to that of the administration of [64Cu]-Cu(atsm) (2.59 ± 0.20%IA/g; $p < 0.06$). The administration of [64Cu]Cu(L²), possessing a pendent N,N-dimethylamino-ethane functional group to mice results in a significantly higher brain uptake than the administration of [64Cu]Cu(atsm), suggesting that the compound has the potential to be used in imaging brain tumors as well as ALS and Parkinson's disease.

■ EXPERIMENTAL SECTION

General Procedures. The following reagents were used as received: spermine (Sigma-Aldrich), butane-1,4-diamine (Sigma-Aldrich), di-tert-butyl dicarbonate (Sigma-Aldrich), N,N-dimethyle-thylenediamine (Aldrich Chemicals), and N-methylethylenediamine (Aldrich Chemicals). All solvents were obtained from standard commercial sources and used as received. NMR spectra were acquired on Varian FT-NMR 500 and FT-NMR 400 spectrometers. ¹H NMR spectra were acquired at 500 or 400 MHz, and ¹³C{¹H} NMR spectra were acquired at 125.7 MHz. All NMR spectra were recorded at 25 °C unless otherwise indicated. ¹H and ¹³C{¹H} chemical shifts were referenced to residual solvent peaks and are quoted in parts per million relative to tetramethylsilane . MS spectra were recorded on an Agilent 6510 ESI-TOF LC/MS mass spectrometer. Cyclic voltammo-grams were recorded on an Autolab PGSTAT100 electrochemical workstation using GPES V4.9 software and employing a glassy carbon working electrode, a platinum counter electrode, and an Ag/Ag⁺ reference electrode [silver wire in CH₃CN (AgNO₃; 0.01 M)]. All measurements were carried out in DMF. All solutions were 5 mM analyte in a 0.1 M tetrabutylammoniumtetrafluoroborate solution. DMF was obtained from commercial sources and dried over 3 Å sieves before use. Each solution was purged with N₂ prior to analysis and measured at ambient temperatures under a N₂ atmosphere. The peak (E_p) and median ($\bar{E}$) potentials were referenced to the Fc/Fc⁺ couple, +0.54 V in DMF versus SCE. The Fc/Fc⁺ median potential under the conditions used was +0.07 V. Microanalyses for carbon, hydrogen, and nitrogen were carried out by Chemical & Micro-analytical Services (CMAS) Pty. Ltd., Belmont, Victoria, Canada. RP-HPLC utilized an Agilent 1200 series HPLC system using an Agilent Zorbax Eclipse XDB-C18 column (4.6 × 150 mm, 5 μm) with a 1 mL/min flow rate, gradient elution of buffer A = 0.1% TFA in H₂O and buffer B = 0.1% TFA in acetonitrile (0−100% B in A at 20 min) and detection at 220, 254, and 275 nm. ⁶⁴Cu was produced via the ⁶⁴Ni(p,n)⁶⁴Cu reaction, using a custom-manufactured solid target assembly positioned externally to a Cyclone 18/9 (IBA) cyclotron. The target consisted of ⁶⁴Ni metal (enriched to 94.8−99.07%) electroplated onto a gold foil (15 mm × 125 μm) backing, housed in a custom-made aluminum cradle. The primary proton beam was degraded to 11.7 MeV using a graphite degrader built into a graphite collimator. Helium cooling was on the target holder at beam entry and chilled water upon beam exit. All targets were irradiated at 40 μA, for up to 2 h. After irradiation, the target was transferred to the laboratory for further chemical processing, in which ⁶⁴Cu was isolated using ion-exchange chromatography using low concentrations of HCl in alcohol solutions. Final reconstitution of the ⁶⁴Cu fraction in

aqueous HCl yielded 1–2.6 GBq of ^{64}Cu as ^{64}CuCl$_2$ (specific activity, 28.9 GBq μmol^{-1} (μA·h/mg of ^{64}Ni)$^{-1}$; radionuclidic purity, 99%).

Cu(atsm) and H$_2$L^1, H$_2$L^3, Cu(L^3), [H$_3$L^4][CF$_3$CO$_2$], and [Cu(H$_2$L^4)][CF$_3$CO$_2$]$_2$ were prepared as previously published.[45]

Synthesis. Diacetyl-4-ethylenedimethylamine-4′-methylbis-(thiosemicarbazone), H$_2$L^2. To a stirring suspension of H$_2$L^1 (0.21 g, 0.85 mmol) in acetonitrile (30 mL) was added *N*-dimethylethylenediamine (0.01 g, 1.12 mmol). The resulting yellow suspension was heated at reflux for 6.5 h under an atmosphere of N$_2$. The resulting orange solution was cooled to room temperature, resulting in the precipitation of colorless crystals, which were collected by filtration, washed with acetonitrile (1×) and diethyl ether (3×), and dried to give H$_2$L^2 (0.18 g, 0.55 mmol, 74%). Elem anal. Found: C, 41.69; H, 7.36; N, 30.74. Calcd for C$_{11}$H$_{23}$N$_7$S$_2$: C, 41.61; H, 7.30; N, 30.88. ^{1}H NMR (DMSO-d_6, 500 MHz): δ 2.16, 3H, s, CH$_3$; 2.19, 6H, s, CH$_3$; 2.21, 3H, s, CH$_3$; 2.46, 2H, t, $^3J_{HH}$ = 6.5 Hz, CH$_2$; 3.03, 3H, d, $^3J_{HH}$ = 4 Hz, NHCH$_3$; 3.61, 2H, m, CH$_2$; 8.34–8.37, 2H, m, NHCH$_2$, NHCH$_3$; 10.24, 2H, br s, NH. ^{13}C{^{1}H} NMR (125.7 MHz): δ 11.3, 11.7, CH$_3$; 31.2, NHCH$_3$; 41.4, CH$_2$; 45.0, N(CH$_3$)$_2$; 57.1, CH$_2$; 147.5, 147.9, C=N; 177.6, 178.5, C=S. ESI-MS (positive ion; 100%, [M + H$^+$]): *m/z* 318.15 (experimental), 318.15 (calcd). RP-HPLC: R_T = 7.58 min.

Diacetyl-4-ethylenedimethylamine-4′-methylbis-(thiosemicarbazonato)copper(II), Cu(L^2). To a solution of H$_2$L^2 (0.10 g, 0.3 mmol) in acetonitrile (10 mL) was added Cu(OAc)$_2$·H$_2$O (0.07 g, 0.3 mmol), and the resulting red/brown suspension was stirred at reflux for 1.5 h and then allowed to cool to room temperature. The solid was collected by filtration, washed with acetonitrile (1×) and diethyl ether (3×), and dried to give Cu(L^2) (0.09 g, 75%). Elem anal. Found: C, 34.87; H, 5.62; N, 25.79. Calcd for C$_{11}$H$_{21}$CuN$_7$S$_2$: C, 34.86; H, 5.58; N, 25.87. ESI-MS: (positive ion; 100%, [M + H$^+$]): *m/z* 379.07 (experimental), 379.07 (calcd). RP-HPLC: R_T = 7.67 min.

tert-Butyl Methyl[2-(2,2,2-trifluoroacetylamino)ethyl]-carbamate. The title compound was prepared according to a literature procedure and isolated as a white crystalline solid (3.90 g, 72%).[49] ^{1}H NMR (CDCl$_3$, 500 MHz): δ 1.46, 9H, s, (CH$_3$)$_3$; 2.90, 3H, s, CH$_3$; 3.48, 4H, br m, CH$_2$; 7.95, br s, NH.

tert-Butyl (2-Aminoethyl)methylcarbamate. The title compound was prepared according to a literature procedure and isolated as a yellow oil (1.71 g, 68%).[49] ^{1}H NMR (CDCl$_3$, 500 MHz): δ 1.45, 9H, s, (CH$_3$)$_3$; 2.82, 2H, t, NH$_2$CH$_2$; 2.87, 3H, s, CH$_3$; 3.27, br m, 2H, CH$_2$.

tert-Butyl 4-Aminobutylcarbamate. The title compound was prepared according to a literature procedure and isolated as a colorless oil.[56] ^{1}H NMR (CDCl$_3$, 500 MHz): δ 1.43, 9H, s, (CH$_3$)$_3$; 1.45–1.53, 4H, m, CH$_2$; 2.70, 2H, t, $^3J_{HH}$ = 7 Hz, CH$_2$; 3.12, 2H, q, $^3J_{HH}$ = 6 Hz, CH$_2$.

(N^1,N^4,N^9-Tri-tert-butoxycarbonyl)-N,N′-bis(3-aminopropyl)-butane-1,4-diamine. The title compound was prepared according to a literature procedure and obtained as a colorless, homogeneous oil (1.33 g, 51%), R_f 0.5 [CH$_2$Cl$_2$–MeOH–concentrated aqueous NH$_3$, 5:1:0.1 (v/v/v)] after purification over silica gel [CH$_2$Cl$_2$–MeOH–concentrated aqueous NH$_3$, 100:0:0 to 5:1:0.1 (v/v/v)].[57] ^{1}H NMR (CDCl$_3$, 500 MHz): δ 1.42–1.50, 31H, m, CH$_3$ × 3, CH$_2$ × 2; 1.61–1.67, 4H, m, CH$_2$ × 2; 3.08–3.31, 10H, m, CH$_2$ × 5. ESI-MS (positive ion; 100%, [M + H$^+$]): *m/z* 503.41 (experimental), 503.41 (calcd).

Diacetyl-tert-butyl-4-ethylmethylcarbamate-4′-methylbis-(thiosemicarbazone), H$_2$L^5·0.5CH$_3$CN. Following the same procedure employed for the synthesis of H$_2$L^2, H$_2$L^1 (0.55 g, 2.0 mmol) and *tert*-butyl (2-aminoethyl)methylcarbamate (0.42 g, 2.4 mmol) were used to prepare H$_2$L^5 (0.70 g, 86%). Elem anal. Found: C, 45.30; H, 7.17; N, 25.00. Calcd for C$_{15}$H$_{29}$N$_7$O$_2$S$_2$·0.5CH$_3$CN: C, 45.31; H, 7.25; N, 24.77. ^{1}H NMR (DMSO-d_6, 500 MHz, 343 K): δ 1.38, 9H, s, (CH$_3$)$_3$; 2.05, CH$_3$CN; 2.21, 3H, s, CH$_3$; 2.22, 3H, s, CH$_3$; 2.84, 3H, s, CH$_3$; 3.05, 3H, d, $^3J_{HH}$ = 4.5 Hz, NHCH$_3$; 3.43, 2H, t, $^3J_{HH}$ = 6.0 Hz, CH$_2$; 3.71–3.77, 2H, m, NHCH$_2$, NHCH$_3$; 8.25–8.35, 2H, br m, NHCH$_2$, NHCH$_3$; 10.07, 2H, s, NH. ^{13}C{^{1}H} NMR (125.7 MHz, 343 K): δ 11.2, 11.3, CH$_3$; 27.8, (CH$_3$)$_3$; 30.9, NHCH$_3$; 34.0, NCH$_3$; 42.0, CH$_2$; 46.8,

CH$_2$; 78.3, C(CH$_3$)$_3$; 147.4, 147.8, C=N; 155.0, C=O; 178.1, 178.6, C=S. ESI-MS (positive ion; 100%, [M + H$^+$]): *m/z* 404.19 (experimental), 404.19 (calcd).

Diacetyl-tert-butyl-4-ethylmethylcarbamate-4′-methylbis-(thiosemicarbazonato)copper(II), Cu(L^5)·H$_2$O. To a solution of H$_2$L^5 (0.18 g, 0.5 mmol) in ethanol (10 mL) was added Cu(OAc)$_2$·H$_2$O (0.10 g, 0.5 mmol), and the resulting red/brown suspension was stirred at reflux for 2 h. The solvent was removed in vacuo, and the brown residue was dissolved in acetone (3 mL) and precipitated with hexane (30 mL). The solid was collected by filtration, washed with hexane, and dried to give Cu(L^5) (0.16 g, 78%). Elem anal. Found: C, 36.84; H, 5.51; N, 19.82. Calcd for C$_{15}$H$_{27}$CuN$_7$O$_2$S$_2$·H$_2$O: C, 37.29; H, 6.05; N, 20.29. ESI-MS (positive ion; 100%, [M + H$^+$]): *m/z* 465.10 (experimental), 465.10 (calcd). RP-HPLC: R_T = 13.01 min.

Diacetyl-4-ethylenemethylaminium-4′-methylbis-(thiosemicarbazone) Trifluoroacetate, [H$_3$L^6][CF$_3$CO$_2$]. A solution of H$_2$L^5(0.11 g, 0.3 mmol) in CH$_2$Cl$_2$ (4 mL) was added dropwise over 20 min to TFA (4 mL) with stirring in an ice bath. The resulting solution was left to warm to room temperature before the solvent was removed in vacuo. To the orange oily residue was added diethyl ether (25 mL), resulting in a precipitate, which was collected by filtration, washed with diethyl ether, and dried to give [H$_3$L^6][CF$_3$CO$_2$] as a white solid (0.09 g, 0.22 mmol). Elem anal. Found: C, 34.46; H, 5.21; N, 23.35. Calcd for C$_{12}$H$_{22}$F$_3$N$_7$O$_2$S$_2$: C, 34.52; H, 5.31; N, 23.49. ^{1}H NMR (DMSO-d_6, 500 MHz): δ 2.23, 6H, s, CH$_3$; 2.61, 3H, s, CH$_3$; 3.02, 3H, d, CH$_3$; 3.16, 2H, br, CH$_2$; 3.89, br, 2H, CH$_2$; 8.40, 1H, br, NH; 8.50, br, 3H, NH, NH$_2$$^+CH_3$; 10.25, s, 1H, NH; 10.54, s, 1H, NH. ^{13}C{^{1}H} NMR (125.7 MHz): δ 11.7, 11.9, CH$_3$; 31.2, CH$_3$; 32.9, CH$_3$; 40.5, 47.5, CH$_2$; 117.2, q, $^1J_{CF}$ = 299.5 Hz, CF$_3$; 147.7, 148.9, C=N; 158.2, q, $^2J_{CF}$ = 31.3 Hz, CCF$_3$; 178.5, C=S. ESI-MS (positive ion; 100%, [M + H$^+$]): *m/z* 304.14 (experimental), 304.14 (calcd).

Diacetyl-4-ethylenemethylaminium-4′-methylbis-(thiosemicarbazonato)copper(II) Trifluoroacetate, [Cu(HL^6)]-[CF$_3$CO$_2$]·0.8CF$_3$CO$_2$H. To a solution of trifluoroacetic acid (5 mL, 0 °C) cooled in an ice bath was added Cu(L^5) (0.07 g, 0.14 mmol) in portions over 20 min. The solution mixture was warmed to room temperature and stirred for 1.5 h. The solvent was removed in vacuo to give a brown oil. Diethyl ether was added, and a brown solid precipitated, which was collected by filtration, washed with diethyl ether, and dried to give [Cu(HL^6)][CF$_3$CO$_2$]·0.8CF$_3$CO$_2$H (0.05 g, 65%). Elem anal. Found: C, 28.38; H, 3.87; N, 17.49. Calcd for C$_{12}$H$_{19}$CuF$_3$N$_7$O$_2$S$_2$·0.8C$_2$HF$_3$O$_2$: C, 28.65; H, 3.68; N, 17.19. ESI-MS (positive ion; 100%, [M + H$^+$]): *m/z* 365.05 (experimental), 365.05 (calcd). RP-HPLC: R_T = 7.42 min.

Diacetyl tert-Butyl-4-butylcarbamate-4′-methylbis-(thiosemicarbazone), H$_2$L^7. Following the same procedure that was employed for the synthesis of H$_2$L^2, H$_2$L^1 (0.20 g, 0.74 mmol) and *tert*-butyl 4-aminobutylcarbamate (0.21 g, 1.1 mmol) were used to prepare H$_2$L^7 (0.27 g, 87%). Elem anal. Found: C, 45.63; H, 7.56; N, 23.31. Calcd for C$_{16}$H$_{31}$N$_7$O$_2$S$_2$: C, 46.02; H, 7.48; N, 23.48. ^{1}H NMR (DMSO-d_6, 500 MHz): δ 1.35–1.42, 11H, br, (CH$_3$)$_3$, CH$_2$; 1.54, 2H, m, CH$_2$; 2.20, 6H, s, CH$_3$; 2.93, 2H, m, CH$_2$; 3.02, 3H, d, $^3J_{HH}$ = 6 Hz, NHCH$_3$; 3.55, 2H, m, CH$_2$; 6.77, 1H, s, NHCO; 8.35–8.40, 2H, br m, NHCH$_3$, NHCH$_2$; 10.13, 2H, br s, NH. ^{13}C{^{1}H} NMR (125.7 MHz): δ 11.6, 11.7, CH$_3$; 26.2, CH$_2$; 27.0, CH$_2$; 28.3, (CH$_3$)$_3$; 31.2, CH$_3$NH; 40.2, CH$_2$; 43.5, CH$_2$; 77.3, C(CH$_3$)$_3$; 147.8, 148.0, C=N; 155.6, C=O; 177.6, 178.5, C=S. ESI-MS (positive ion; 100%, [M + H$^+$]): *m/z* 418.21 (experimental), 418.21 (calcd). RP-HPLC: R_T = 16.40 min.

Diacetyl tert-Butyl-4-butylcarbamate-4′-methylbis-(thiosemicarbazonato)copper(II), Cu(L^7)·H$_2$O·0.5CH$_3$CN. Following the same procedure that was employed for the synthesis of Cu(L^2), H$_2$L^7 (0.10 g, 0.25 mmol) and Cu(OAc)$_2$·H$_2$O (0.05 g, 0.25 mmol) were used to prepare Cu(L^7) (0.10 g, 81%). (Elem anal. Found: C, 39.25; H, 6.24; N, 20.83. Calcd for C$_{16}$H$_{29}$CuN$_7$O$_2$S$_2$·H$_2$O·0.5CH$_3$CN: C, 39.44; H, 6.33; N, 20.29. ESI-MS (positive ion; 100%, [M + H$^+$]): *m/z* 479.12 (experimental), 479.12 (calcd). RP-HPLC: R_T = 15.13 min.

Diacetyl-4-butyleneaminium-4′-methylbis(thiosemicarbazone) Trifluoroacetate, [HL⁸][CF₃CO₂]. Following the same procedure that was employed for the synthesis of [H₃**L⁶**][CF₃CO₂], H₂**L⁷** (0.06 g, 0.13 mmol) was used to prepare [H**L⁸**][CF₃CO₂] (0.05 g, 86%). Elem anal. Found: C, 36.30; H, 5.71; N, 21.59. Calcd for $C_{13}H_{24}CuN_7F_3O_2S_2$: C, 36.19; H, 5.61; N, 22.72. ¹H NMR (DMSO-d_6, 500 MHz): δ 1.52−1.67, 4H, m, CH₂; 2.21, 6H, s, CH₃; 2.82, 2H, m, CH₂; 3.02, 3H, d, CH₃, $^3J_{HH}$ = 4 Hz; 3.60, m, 2H, CH₂; 7.69, 3H, br s, NH₃⁺; 8.35−8.47, m, 2H, NH; 10.21, br s, 2H, NH. ESI-MS (positive ion; 100%, [M⁺]): *m/z* 318.15 (experimental), 318.15 (calcd). RP-HPLC: R_T = 10.02 min.

Diacetyl-4-butyleneaminium-4′-methylbis(thiosemicarbazonato)copper(II) Trifluoroacetate, [Cu(HL⁸)][CF₃CO₂]. Following the same procedure that was employed for the synthesis of [Cu(H**L⁶**)][CF₃CO₂]·0.8CF₃CO₂H, Cu(**L⁷**) (0.04 g, 0.1 mmol) was used to prepare [Cu(H**L⁸**)][CF₃CO₂] (0.02 g, 51%). Elem anal. Found: C, 31.64; H, 4.56; N, 19.81. Calcd for $C_{13}H_{22}CuN_7F_3O_2S_2$: C, 31.67; H, 4.50; N, 19.89. ESI-MS (positive ion; 100%, [M⁺]): *m/z* 379.07 (experimental), 379.07 (calcd). RP-HPLC: R_T = 7.62 min.

Diacetyl 4-(N¹,N⁴,N⁹-Tri-tert-butoxycarbonyl)-N,N′-bis(3-aminopropyl)butane-1,4-diamine-4′-methylbis(thiosemicarbazone), H₂L⁹. To a stirring suspension of H₂**L¹** (0.30 g, 1.1 mmol) in acetonitrile (20 mL) was added (N¹,N⁴,N⁹-tri-*tert*-butoxycarbonyl)-N,N′-bis(3-aminopropyl)butane-1,4-diamine (0.56 g, 1.1 mmol). The mixture was heated at reflux for 3 h and monitored by thin-layer chromatography analysis [5% MeOH−CH₂Cl₂ (v/v)]. The resulting suspension was cooled to room temperature and filtered to remove the white precipitate. The solvent was removed in vacuo to give a light-yellow, glassy solid, which was purified over silica [CH₂Cl₂−MeOH−Et₃N 100:0:0 to 100:1:0.1 to 100:4:0.1 (v/v/v)] to afford H₂**L⁹** as a white glassy solid (0.66 g, 0.9 mmol, 81%), R_f = 0.6 [5% MeOH−CH₂Cl₂ (v/v)]. Elem anal. Found: C, 52.37; H, 8.46; N, 17.17. Calcd for $C_{32}H_{61}N_9O_6S_2$: C, 52.50; H, 8.40; N, 17.22. ¹H NMR (DMSO-d_6, 500 MHz, 343 K): δ 1.38, 9H, s, (CH₃)₃; 1.39, 9H, s, (CH₃)₃; 1.41, 9H, s, (CH₃)₃; 1.42−1.47, 4H, br m, CH₂⁵, CH₂⁶; 1.59, 2H, p, $^3J_{HH}$ = 7 Hz, CH₂; 1.73−1.81, 2H, br m, CH₂; 2.21, 3H, s, CH₃; 2.22, 2H, s, CH₃; 2.91, 2H, q, $^3J_{HH}$ = 6 Hz, CH₂; 3.05, 3H, d, $^3J_{HH}$ = 4.5 Hz, C*H₃*NH; 3.10−3.17, 6H, m, CH₂, CH₂, CH₂; 3.21, 2H, t, $^3J_{HH}$ = 7 Hz, CH₂; 3.57, 2H, q, $^3J_{HH}$ = 6.5 Hz, CH₂; 6.44−6.60, 1H, br s, NH; 8.28, 1H, m, NHC*H₂*; 8.39−8.60, 1H, br s, NHC*H₂*; 9.95−10.10, 2H, br s, NH. ¹³C{¹H} NMR (125.7 MHz, 343 K): δ 11.1, 11.3, CH₃; 25.3, CH₂; 27.8, 27.8, 28.0, (CH₃)₃, CH₂; 28.5, CH₂; 30.1, C*H₃*NH; 37.5, CH₂; 40.8, CH₂; 43.5, CH₂; 44.2, CH₂; 46.1, CH₂, CH₂; 77.2, 78.0, 78.3, *C*(CH₃)₃; 147.5, 147.7, C═N; 154.4, 155.2, C═O; 177.7, 178.5, C═S. ESI-MS (positive ion; 100%, [M + H⁺]): *m/z* 732.43 (experimental), 732.43 (calcd). RP-HPLC: R_T = 18.16 min.

Diacetyl 4-(N¹,N⁴,N⁹-tri-tert-butoxycarbonyl)-N,N′-bis(3-aminopropyl)butane-1,4-diamine-4′-methylbis(thiosemicarbazonato)copper(II), Cu(L⁹). To a solution of H₂**L⁹** (0.31 g, 0.4 mmol) in ethanol (5 mL) was added Cu(OAc)₂·H₂O (0.09 g, 0.4 mmol). The red/brown solution was stirred at room temperature for 19 h. The solvent was removed in vacuo, and the brown residue was dissolved in dichloromethane (3 mL) and filtered. The solvent was removed in vacuo to give Cu(**L⁹**) as a brown/red glassy solid (0.29 g, 88%). Elem anal. Found: C, 48.38; H, 7.53; N, 15.92. Calcd for $CuC_{32}H_{59}N_9O_6S_2$: C, 48.43; H, 7.49; N, 15.89. ESI-MS (positive ion; 100%, [M + H⁺]): *m/z* 793.34 (experimental), 793.34 (calcd). RP-HPLC: R_T = 17.40 min.

Diacetyl 4-N-(3-Aminiumpropyl)-N′-(3-aminopropyl)butane-1,4-diaminium-4′-methylbis(thiosemicarbazone), [H₅L¹⁰][CF₃CO₂]₃. Following the same procedure that was employed for the synthesis of [H₃**L⁶**][CF₃CO₂], H₂**L⁹** (0.23 g, 0.3 mmol) was used to prepare [H₅**L¹⁰**][CF₃CO₂]₃ (0.22 g, 89%). Elem anal. Found: C, 35.51; H, 5.31; N, 16.20. Calcd for $C_{23}H_{40}F_9N_9O_6S_2$: C, 35.70; H, 5.21; N, 16.29. ¹H NMR (DMSO-d_6, 500 MHz): δ 1.63, 4H, m, CH₂, CH₂; 1.87−1.96, 4H, m, CH₂, CH₂; 2.20, 6H, s, CH₃ × 2; 2.86−3.00, 10H, br, CH₂, CH₂, CH₂, CH₂, CH₂; 3.02, 3H, d, $^3J_{HH}$ = 4.5 Hz, C*H₃*NH; 3.65, 2H, q, $^3J_{HH}$ = 6 Hz, CH₂; 7.98−8.09, 3H, br s, H₃N⁺; 8.39, 1H, q, $^3J_{HH}$ = 4.5 Hz, NHC*H₂*; 8.53, 1H, t, $^3J_{HH}$ = 6 Hz, NHC*H₂*; 8.70−

8.80, 2H, br, H₂N⁺; 8.86−8.95, 2H, br, H₂N⁺; 10.21, 1H, s, NH; 10.30, 1H, s, NH. ¹³C{¹H} NMR (125.7 MHz): δ 11.7, 11.8, CH₃; 22.6, 22.7, CH₂, CH₂; 23.8, CH₂; 25.7, CH₂; 31.2, NHCH₃; 36.2, CH₂; 40.8, CH₂; 43.9, CH₂; 44.7, CH₂; 46.1, 46.2, CH₂, CH₂; 117.0, q, $^1J_{CF}$ = 298.9 Hz, CF₃; 147.8, 148.6, C═N; 158.7, q, $^2J_{CF}$ = 32.0 Hz, *C*CF₃; 178.1, 178.5, C═S. ESI-MS (positive ion; 100%, [M³⁺−2H⁺]): *m/z* 432.27 (experimental), 432.27 (calcd). RP-HPLC: R_T = 6.97 min.

Diacetyl 4-N-(3-Aminiumpropyl)-N′-(3-aminopropyl)butane-1,4-diaminium-4′-methylbis(thiosemicarbazonato)copper(II), [Cu(H₃L¹⁰)][CF₃CO₂]₃·2H₂O. Following the same procedure that was employed for the synthesis of [H₃**L¹⁰**][CF₃CO₂]₃, Cu(**L⁹**) (0.14 g, 0.17 mmol) was used to prepare [Cu(H₃**L¹⁰**)][CF₃CO₂]₃·2H₂O (0.13 g, 89%). Elem anal. Found: C, 31.69; H, 4.43; N, 14.47. Calcd for $C_{23}H_{42}CuF_9N_9O_8S_2$: C, 31.71; H, 4.86; N, 14.47. ESI-MS (positive ion; 100%, [M³⁺− 2H⁺]): *m/z* 493.18 (experimental), 493.18 (calcd). ESI-MS (positive ion; 100%, [M³⁺− H⁺]): *m/z* 247.10 (experimental), 247.10 (calcd). RP-HPLC: R_T = 7.05 min.

Radiochemistry. An aliquot of [⁶⁴Cu]CuCl₂ (95 μL, ∼60 MBq, pH 1) was added to a solution containing the ligand (5 μL, 1 mg/mL DMSO) and PBS (210 μL, 0.1 M). The reaction was left for 30 min at room temperature before 5 μL of the reaction solution was injected onto a C18 analytical RP-HPLC column. A DMSO solution of the nonradioactive copper complex (1 mg/mL) was injected (8 μL) under the same conditions (λ = 275 nm) to verify the identity of the radiolabeled complex. HPLC were performed using a Shimadzu SPD-10ATvP HPLC system equipped with a Phenomenex Luna C18 100 Å column (4.6 × 150 mm, 5 μm) with a 1 mL/min flow rate and with scintillation and UV−vis detectors in series (280 nm). Retention times (R_T/min) were recorded using a gradient elution method of 5−100% B over 10 min; solution A consisted of water (buffered with 0.1% trifluoroacetic acid), and solution B consisted of acetonitrile (buffered with 0.1% trifluoroacetic acid).

Distribution Coefficients. Octanol/water distribution coefficients were measured by vortex mixing 0.5 mL of 1-octanol and 0.5 mL of isotonic PBS (pH 7.4) with a 25−50 μL sample of an aqueous solution of the copper-64 complex. Following centrifugation, 100 μL each of the octanol and aqueous phases was sampled, diluted to 1 mL, and counted in an automatic well counter using a window centered at 511 keV. Distribution coefficients, *D*, are reported as counts per gram of octanol divided by counts per gram of water.

Exposure of Bis(thiosemicarbazonato)copper(II) Complexes to SH-SY5Y Cells and ICP-MS. SH-SY5Y neuroblastoma cells were seeded into 10 cm plates at a density of 5 × 10⁴ cm⁻² and then grown for 4 days before treatment with the Cu(btsc) complexes. At treatment, the cells were ∼90% confluent. The copper complexes were prepared as 10 mM stock solutions in DMSO. CuSO₄ was prepared as a 10 mM stock solution in PBS. An aliquot (50 μL) of the stock solution was added to 50 mL of a DMEM:F12 medium to give a final complex concentration of 10 μM. Existing media were removed from the cells and replaced by the media/copper complex mixture (15 mL/plate). Each compound was treated in triplicate. The cells were incubated for 1 h at 37 °C. The cells were scraped into the media, and then the cells/media mixture was centrifuged at 1000*g* for 3 min to pellet cells. The media were removed, and the cells were resuspended in PBS (pH 7.4) and centrifuged at 1000*g* for 3 min. The cells were again resuspended in PBS, an aliquot was taken for protein determination (Protein Microassay, Bio-Rad), the remaining cells were centrifuged at 3000 rpm for 5 min, and the cell pellets were stored at −70 °C. The metal levels were determined in cell pellets using ICP-MS. An Agilent 7700 series ICP-MS instrument was used under routine multielement operating conditions with a helium reaction gas cell as described previously.[77] Briefly, concentrated nitric acid (65%, 50 μL; Suprapur, Merck) was added to each cell pellet and allowed to digest overnight at ambient temperature. The samples were then heated at 90 °C for 25 min using a heating block to complete the digestion. To each sample was added 1% (v/v) nitric acid (1.0 mL). The metal content of the samples was calculated relative to the sample protein content and then converted to a fold increase in the cellular

metal compared with vehicle-treated controls. The data are the mean ± standard error of the mean (SEM) from triplicate samples.

LDH and MTT Cytotoxicity Assays. SH-SY5Y cells were cultured as above. After 4 days of growth, once the cultures had reached 90% confluency, cultures were treated with Cu(btsc) complexes at concentrations of 0, 1.25, 2.5, 5, and 10 μM for 1 h. The LDH and MTT assays were performed as previously described.[61−63] The spectrophotometric absorbance was 490 nm for the LDH assay and 560 nm for the MTT assay. The relative % LDH release was calculated by treating some cells with the detergent Triton X-100, which was added to the media to a final concentration of 1% v/v to permeabilize the cells. This treatment completely permeabilizes the cell membranes and therefore induces the total release of cellular LDH into the media (100% LDH release). Relative % MTT reduction was calculated relative to vehicle-treated cells (100% MTT reduction). All absorbance readings for the LDH and MTT assays were adjusted using relevant controls (i.e., absorbance values for cell-free media were subtracted).

Small-Animal PET Imaging and Biodistribution Studies. All mouse experiments were performed with approval from the Peter MacCallum Cancer Centre Animal Experimentation Ethics Committee. For brain imaging studies, Balb/c mice were anaesthetized using isoflurane in 50% oxygen in air before being injected intravenously with 15−20 MBq of activity. The animals were then placed on the bed of a Philips Mosaic small-animal PET scanner 5 min postinjection and imaged over 10 min. The PET images were reconstructed using a 3D RAMLA algorithm as described previously.[78] For the A431 xenograft model, female Balb/C nude mice were injected subcutaneously on the right flank with 3×10^6 of A431 cells. Once the tumors reached a volume of 250−500 mm^3, the mice were assigned to two groups of three mice and injected with either [^{64}Cu]Cu(L^2) or [^{64}Cu]Cu(atsm) (10−15 MBq) via intravenous tail vein injection. Animals were imaged as described previously at 1, 3, and 22 h after tracer injection. The images were reconstructed using a 3D RAMLA algorithm as described previously.[78] Following the final scan, the mice were euthanized and tissues excised for ex vivo biodistribution analysis. Data are presented as mean ± standard error. The statistical significance was determined using two-tailed unpaired *t* tests with Welch's correction.

ASSOCIATED CONTENT

Ⓢ Supporting Information

The Supporting Information is available free of charge on the ACS Publications website at DOI: 10.1021/acs.inorgchem.9b00117.

Portion of the ^{13}C{^{1}H} NMR spectra of H$_2$L^5 at 25 and 70 °C and the s-cis/s-trans equilibrium and double-bond character of the carbamate bond of H$_2$L^5 (PDF)

AUTHOR INFORMATION

Corresponding Author

*E-mail: pauld@unimelb.edu.au.

ORCID Ⓘ

Brett M. Paterson: 0000-0002-7768-811X
Paul S. Donnelly: 0000-0001-5373-0080

Present Addresses

§B.M.P.: School of Chemistry, Monash University, Clayton, Victoria 3800, Australia.
○A.R.W.: QIMR Berghofer Medical Research Institute, Brisbane 4006, Australia.

Author Contributions

The manuscript was written through contributions of all authors. All authors have given approval to the final version of the manuscript.

REFERENCES

(1) Paterson, B. M.; Donnelly, P. S. Copper complexes of bis(thiosemicarbazones): from chemotherapeutics to diagnostic and therapeutic radiopharmaceuticals. *Chem. Soc. Rev.* **2011**, *40*, 3005−3018.

(2) Vavere, A. L.; Lewis, J. S. Cu-ATSM: A radiopharmaceutical for the PET imaging of hypoxia. *Dalton Trans.* **2007**, 4893−4902.

(3) Fujibayashi, Y.; Taniuchi, H.; Yonekura, Y.; Ohtani, H.; Konishi, J.; Yokoyama, A. Copper-62-ATSM: a new hypoxia imaging agent with high membrane permeability and low redox potential. *J. Nucl. Med.* **1997**, *38*, 1155−1160.

(4) Dearling, J. L. J.; Lewis, J. S.; Mullen, G. E. D.; Rae, M. T.; Zweit, J.; Blower, P. J. Design of hypoxia-targeting radiopharmaceuticals: selective uptake of copper-64 complexes in hypoxic cells in vitro. *Eur. J. Nucl. Med. Mol. Imaging* **1998**, *25*, 788−792.

(5) Dearling, J. L. J.; Blower, P. J. Redox-active metal complexes for imaging hypoxic tissues: structure-activity relationships in copper(II) bis(thiosemicarbazone) complexes. *Chem. Commun.* **1998**, 2531−2532.

(6) Lewis, J. S.; McCarthy, D. W.; McCarthy, T. J.; Fujibayashi, Y.; Welch, M. J. Evaluation of ^{64}Cu-ATSM in vitro and in vivo in a hypoxic tumor model. *J. Nucl. Med.* **1999**, *40*, 177−183.

(7) Lewis, J. S.; Laforest, R.; Dehdashti, F.; Grigsby, P. W.; Welch, M. J.; Siegel, B. A. An imaging comparison of ^{64}Cu-ATSM and ^{60}Cu-ATSM in cancer of the uterine cervix. *J. Nucl. Med.* **2008**, *49*, 1177−82.

(8) Dehdashti, F.; Mintun, M. A.; Lewis, J. S.; Bradley, J.; Govindan, R.; Laforest, R.; Welch, M. J.; Siegel, B. A. In vivo assessment of tumor hypoxia in lung cancer with 60Cu-ATSM. *Eur. J. Nucl. Med. Mol. Imaging* **2003**, *30*, 844−850.

(9) Dehdashti, F.; Grigsby, P. W.; Lewis, J. S.; Laforest, R.; Siegel, B. A.; Welch, M. Assessing tumor hypoxia in cervical cancer by PET with ^{60}Cu-labeled diacetyl-bis(N4-methylthiosemicarbazone). *J. Nucl. Med.* **2008**, *49*, 201−205.

(10) Lewis, J. S.; Laforest, R.; Buettner, T. L.; Song, S.-K.; Fujibayashi, Y.; Connett, J. M.; Welch, M. J. Copper-64-diacetyl-bis(N4-methylthiosemicarbazone): an agent for radiotherapy. *Proc. Natl. Acad. Sci. U. S. A.* **2001**, *98*, 1206−1211.

(11) Xiao, Z.; Donnelly, P. S.; Zimmermann, M.; Wedd, A. G. Transfer of Copper between Bis(thiosemicarbazone) Ligands and Intracellular Copper-Binding Proteins. Insights into Mechanisms of Copper Uptake and Hypoxia Selectivity. *Inorg. Chem.* **2008**, *47*, 4338−4347.

(12) Donnelly, P. S.; Liddell, J. R.; Lim, S.; Paterson, B. M.; Cater, M. A.; Savva, M. S.; Mot, A. I.; James, J. L.; Trounce, I. A.; White, A. R.; Crouch, P. J. An impaired mitochondrial electron transport chain increases retention of the hypoxia imaging agent diacetylbis(4-methylthiosemicarbazonato)copperII. *Proc. Natl. Acad. Sci. U. S. A.* **2012**, *109*, 47−52.

(13) Laforest, R.; Dehdashti, F.; Lewis, J. S.; Schwarz, S. W. Dosimetry of 60/61/62/64Cu-ATSM: a hypoxia imaging agent for PET. *Eur. J. Nucl. Med. Mol. Imaging* **2005**, *32*, 764−770.

(14) Ikawa, M.; Okazawa, H.; Arakawa, K.; Kudo, T.; Kimura, H.; Fujibayashi, Y.; Kuriyama, M.; Yoneda, M. PET imaging of redox and energy states in stroke-like episodes of MELAS. *Mitochondrion* **2009**, *9*, 144−148.

(15) Ikawa, M.; Okazawa, H.; Kudo, T.; Kuriyama, M.; Fujibayashi, Y.; Yoneda, M. Evaluation of striatal oxidative stress in patients with Parkinson's disease using [⁶²Cu]ATSM PET. *Nucl. Med. Biol.* **2011**, *38*, 945−951.

(16) Ikawa, M.; Okazawa, H.; Tsujikawa, T.; Matsunaga, A.; Yamamura, O.; Mori, T.; Hamano, T.; Kiyono, Y.; Nakamoto, Y.; Yoneda, M. Increased oxidative stress is related to disease severity in the ALS motor cortex: A PET study. *Neurology* **2015**, *84*, 2033−2039.

(17) Hung, L. W.; Villemagne, V. L.; Cheng, L.; Sherratt, N. A.; Ayton, S.; White, A. R.; Crouch, P. J.; Lim, S.; Leong, S. L.; Wilkins, S.; George, J.; Roberts, B. R.; Pham, C. L. L.; Liu, X.; Chiu, F. C. K.; Shackleford, D. M.; Powell, A. K.; Masters, C. L.; Bush, A. I.; O'Keefe, G.; Culvenor, J. G.; Cappai, R.; Cherny, R. A.; Donnelly, P. S.; Hill, A. F.; Finkelstein, D. I.; Barnham, K. J. The hypoxia imaging agent Cu^{II}(atsm) is neuroprotective and improves motor and cognitive functions in multiple animal models of Parkinson's disease. *J. Exp. Med.* **2012**, *209*, 837−854.

(18) Soon, C. P. W.; Donnelly, P. S.; Turner, B. J.; Hung, L. W.; Crouch, P. J.; Sherratt, N. A.; Tan, J. L.; Lim, N. K. H.; Lam, L.; Bica, L.; Lim, S. C.; Hickey, J. L.; Morizzi, J.; Powell, A.; Finkelstein, D. I.; Culvenor, J. G.; Masters, C. L.; Duce, J.; White, A. R.; Barnham, K. J.; Li, Q. X. Diacetylbis(N(4)-methylthiosemicarbazonato) Copper(II) (Cu^{II}(atsm)) Protects against Peroxynitrite-induced Nitrosative Damage and Prolongs Survival in Amyotrophic Lateral Sclerosis Mouse Model. *J. Biol. Chem.* **2011**, *286*, 44035−44044.

(19) Parker, S. J.; Meyerowitz, J.; James, J. L.; Liddell, J. R.; Nonaka, T.; Hasegawa, M.; Kanninen, K. M.; Lim, S. C.; Paterson, B. M.; Donnelly, P. S.; Crouch, P. J.; White, A. R. Inhibition of TDP-43 accumulation by Bis(thiosemicarbazonato)-copper complexes. *PLoS One* **2012**, *7*, No. e42277.

(20) McAllum, E. J.; Lim, N. K. H.; Hickey, J. L.; Paterson, B. M.; Donnelly, P. S.; Li, Q.-X.; Liddell, J. R.; Barnham, K. J.; White, A. R.; Crouch, P. J. Therapeutic effects of Cu^{II}(atsm) in the SOD1-G37R mouse model of amyotrophic lateral sclerosis. *Amyotrophic Lateral Scler. Frontotemporal Degener.* **2013**, *14*, 586−590.

(21) Roberts, B. R.; Turner, B. J.; Bush, A. I.; Masters, C. L.; Li, Q.-X.; Lim, N. K. H.; McAllum, E. J.; Price, K. A.; Kanninen, K. M.; Liddell, J. R.; Grubman, A.; Donnelly, P. S.; Chun Lim, S.; Paterson, B. M.; Hickey, J. L.; Hare, D. J.; Doble, P. A.; Rhoads, T. W.; Williams, J. R.; Hung, L. W.; Monty, J.-F.; Llanos, R. M.; Mercer, J. F. B.; Kramer, D. R.; Duce, J. A.; Beckman, J. S.; Barnham, K. J.; White, A. R.; Crouch, P. J. Oral Treatment with CuII(atsm) Increases Mutant SOD1 In Vivo but Protects Motor Neurons and Improves the Phenotype of a Transgenic Mouse Model of Amyotrophic Lateral Sclerosis. *J. Neurosci.* **2014**, *34*, 8021−8031.

(22) McAllum, E. J.; Roberts, B. R.; Hickey, J. L.; Dang, T. N.; Grubman, A.; Donnelly, P. S.; Liddell, J. R.; White, A. R.; Crouch, P. J. Zn^{II}(atsm) is protective in amyotrophic lateral sclerosis model mice via a copper delivery mechanism. *Neurobiol. Dis.* **2015**, *81*, 20−24.

(23) Hilton, J. B.; Mercer, S. W.; Lim, N. K. H.; Faux, N. G.; Buncic, G.; Beckman, J. S.; Roberts, B. R.; Donnelly, P. S.; White, A. R.; Crouch, P. J. Cu^{II}(atsm) improves the neurological phenotype and survival of SOD1G93A mice and selectively increases enzymatically active SOD1 in the spinal cord. *Sci. Rep.* **2017**, *7*, 42292.

(24) John, E. K.; Green, M. A. Structure-activity relationships for metal-labeled blood flow tracers: comparison of keto aldehyde bis(thiosemicarbazonato)copper(II) derivatives. *J. Med. Chem.* **1990**, *33*, 1764−70.

(25) Price, K. A.; Crouch, P. J.; Volitakis, I.; Paterson, B. M.; Lim, S.; Donnelly, P. S.; White, A. R. Mechanisms Controlling the Cellular Accumulation of Copper Bis(thiosemicarbazonato) Complexes. *Inorg. Chem.* **2011**, *50*, 9594−9605.

(26) Green, M. A.; Klippenstein, D. L.; Tennison, J. R. Copper(II) bis(thiosemicarbazone) complexes as potential tracers for evaluation of cerebral and myocardial blood flow with PET. *J. Nucl. Med.* **1988**, *29*, 1549−57.

(27) Bayly, S. R.; King, R. C.; Honess, D. J.; Barnard, P. J.; Betts, H. M.; Holland, J. P.; Hueting, R.; Bonnitcha, P. D.; Dilworth, J. R.; Aigbirhio, F. I.; Christlieb, M. In vitro and in vivo evaluations of a hydrophilic ⁶⁴Cu-bis(thiosemicarbazonato)-glucose conjugate for hypoxia imaging. *J. Nucl. Med.* **2008**, *49*, 1862−1868.

(28) Holland, J. P.; Aigbirhio, F. I.; Betts, H. M.; Bonnitcha, P. D.; Burke, P.; Christlieb, M.; Churchill, G. C.; Cowley, A. R.; Dilworth, J. R.; Donnelly, P. S.; Green, J. C.; Peach, J. M.; Vasudevan, S. R.; Warren, J. E. Functionalized Bis(thiosemicarbazonato) Complexes of Zinc and Copper: Synthetic Platforms Toward Site-Specific Radiopharmaceuticals. *Inorg. Chem.* **2007**, *46*, 465−485.

(29) Buncic, G.; Hickey, J. L.; Schieber, C.; White, J. M.; Crouch, P. J.; White, A. R.; Xiao, Z.; Wedd, A. G.; Donnelly, P. S. Water-soluble Bis(thiosemicarbazonato)copper(II) Complexes. *Aust. J. Chem.* **2011**, *64*, 244−252.

(30) Hickey, J. L.; Crouch, P. J.; Mey, S.; Caragounis, A.; White, J. M.; White, A. R.; Donnelly, P. S. Copper(II) complexes of hybrid hydroxyquinoline-thiosemicarbazone ligands: GSK3β inhibition due to intracellular delivery of copper. *Dalton Trans.* **2011**, *40*, 1338−1347.

(31) Poduslo, J. F.; Curran, G. L.; Gill, J. S. Putrescine-modified nerve growth factor: bioactivity, plasma pharmacokinetics, blood-brain/nerve barrier permeability, and nervous system biodistribution. *J. Neurochem.* **1998**, *71*, 1651−1660.

(32) Zhang, L.; Lee, H.-K.; Pruess, T. H.; White, H. S.; Bulaj, G. Synthesis and applications of polyamine amino acid residues: improving the bioactivity of an analgesic neuropeptide, neurotensin. *J. Med. Chem.* **2009**, *52*, 1514−1517.

(33) Zorko, M.; Langel, U. Cell-penetrating peptides: mechanism and kinetics of cargo delivery. *Adv. Drug Delivery Rev.* **2005**, *57*, 529−545.

(34) Phanstiel, O.; Kaur, N.; Delcros, J. G. Structure-activity investigations of polyamine-anthracene conjugates and their uptake via the polyamine transporter. *Amino Acids* **2007**, *33*, 305−313.

(35) Delcros, J.-G.; Tomasi, S.; Duhieu, S.; Foucault, M.; Martin, B.; Le Roch, M.; Eifler-Lima, V.; Renault, J.; Uriac, P. Effect of polyamine homologation on the transport and biological properties of heterocyclic amidines. *J. Med. Chem.* **2006**, *49*, 232−245.

(36) Wang, C.; Delcros, J.-G.; Biggerstaff, J.; Phanstiel, O. Synthesis and Biological Evaluation of N1-(Anthracen-9-ylmethyl)triamines as Molecular Recognition Elements for the Polyamine Transporter. *J. Med. Chem.* **2003**, *46*, 2663−2671.

(37) Barret, J.-M.; Kruczynski, A.; Vispe, S.; Annereau, J.-P.; Brel, V.; Guminski, Y.; Delcros, J.-G.; Lansiaux, A.; Guilbaud, N.; Imbert, T.; Bailly, C. F14512, a Potent Antitumor Agent Targeting Topoisomerase II Vectored into Cancer Cells via the Polyamine Transport System. *Cancer Res.* **2008**, *68*, 9845−9853.

(38) Delcros, J.-G.; Tomasi, S.; Carrington, S.; Martin, B.; Renault, J.; Blagbrough, I. S.; Uriac, P. Effect of Spermine Conjugation on the Cytotoxicity and Cellular Transport of Acridine. *J. Med. Chem.* **2002**, *45*, 5098−5111.

(39) Holley, J. L.; Mather, A.; Wheelhouse, R. T.; Cullis, P. M.; Hartley, J. A.; Bingham, J. P.; Cohen, G. M. Targeting of tumor cells and DNA by a chlorambucil-spermidine conjugate. *Cancer Res.* **1992**, *52*, 4190−5.

(40) Bergeron, R. J.; McManis, J. S.; Weimar, W. R.; Schreier, K.; Gao, F.; Wu, Q.; Ortiz-Ocasio, J.; Luchetta, G. R.; Porter, C.; Vinson, J. R. T. The role of charge in polyamine analog recognition. *J. Med. Chem.* **1995**, *38*, 2278−85.

(41) Wolf, M.; Hull, W. E.; Mier, W.; Heiland, S.; Bauder-Wuest, U.; Kinscherf, R.; Haberkorn, U.; Eisenhut, M. Polyamine-Substituted Gadolinium Chelates: A New Class of Intracellular Contrast Agents for Magnetic Resonance Imaging of Tumors. *J. Med. Chem.* **2007**, *50*, 139−148.

(42) Agostinelli, E.; Marques, M. P. M.; Calheiros, R.; Gil, F. P. S. C.; Tempera, G.; Viceconte, N.; Battaglia, V.; Grancara, S.; Toninello, A. Polyamines: fundamental characters in chemistry and biology. *Amino Acids* **2010**, *38*, 393−403.

(43) Casero, R. A.; Woster, P. M. Recent Advances in the Development of Polyamine Analogues as Antitumor Agents. *J. Med. Chem.* **2009**, *52*, 4551−4573.

(44) Fardin, P.; Barla, A.; Mosci, S.; Rosasco, L.; Verri, A.; Versteeg, R.; Caron, H. N.; Molenaar, J. J.; Øra, I.; Eva, A.; Puppo, M.; Varesio, L. A biology-driven approach identifies the hypoxia gene signature as a predictor of the outcome of neuroblastoma patients. *Mol. Cancer* **2010**, *9*, 185.

(45) Paterson, B. M.; Karas, J. A.; Scanlon, D. B.; White, J. M.; Donnelly, P. S. Versatile New Bis(thiosemicarbazone) Bifunctional Chelators: Synthesis, Conjugation to Bombesin(7−14)-NH2, and Copper-64 Radiolabeling. *Inorg. Chem.* **2010**, *49*, 1884−1893.

(46) Buncic, G.; Donnelly, P. S.; Paterson, B. M.; White, J. M.; Zimmermann, M.; Xiao, Z.; Wedd, A. G. A Water-soluble bis-(thiosemicarbazone) ligand. A sensitive probe and metal buffer for zinc. *Inorg. Chem.* **2010**, *49*, 3071−3073.

(47) Hickey, J. L.; James, J. L.; Henderson, C. A.; Price, K. A.; Mot, A. I.; Buncic, G.; Crouch, P. J.; White, J. M.; White, A. R.; Smith, T. A.; Donnelly, P. S. Intracellular Distribution of Fluorescent Copper and Zinc Bis(thiosemicarbazonato) Complexes Measured with Fluorescence Lifetime Spectroscopy. *Inorg. Chem.* **2015**, *54*, 9556−9567.

(48) Xie, D.; Kim, S.; Kohli, V.; Banerjee, A.; Yu, M.; Enriquez, J. S.; Luci, J. J.; Que, E. L. Hypoxia-Responsive ^{19}F MRI Probes with Improved Redox Properties and Biocompatibility. *Inorg. Chem.* **2017**, *56*, 6429−6437.

(49) Martins, E. T.; Baruah, H.; Kramarczyk, J.; Saluta, G.; Day, C. S.; Kucera, G. L.; Bierbach, U. Design, Synthesis, and Biological Activity of a Novel Non-Cisplatin-type Platinum-Acridine Pharmacophore. *J. Med. Chem.* **2001**, *44*, 4492−4496.

(50) Cox, C.; Lectka, T. Solvent effects on the barrier to rotation in carbamates. *J. Org. Chem.* **1998**, *63*, 2426−2427.

(51) Rablen, P. R. Computational Analysis of the Solvent Effect on the Barrier to Rotation about the Conjugated C-N Bond in Methyl N,N-Dimethylcarbamate. *J. Org. Chem.* **2000**, *65*, 7930−7937.

(52) Stewart, W. E.; Siddall, T. H., III Nuclear magnetic resonance studies of amides. *Chem. Rev.* **1970**, *70*, 517−51.

(53) Scherer, G.; Kramer, M. L.; Schutkowski, M.; Reimer, U.; Fischer, G. Barriers to Rotation of Secondary Amide Peptide Bonds. *J. Am. Chem. Soc.* **1998**, *120*, 5568−5574.

(54) Deetz, M. J.; Forbes, C. C.; Jonas, M.; Malerich, J. P.; Smith, B. D.; Wiest, O. Unusually Low Barrier to Carbamate C-N Rotation. *J. Org. Chem.* **2002**, *67*, 3949−3952.

(55) Smith, B. D.; Goodenough-Lashua, D. M.; D'Souza, C. J. E.; Norton, K. J.; Schmidt, L. M.; Tung, J. C. Substituent effects on the barrier to carbamate C-N rotation. *Tetrahedron Lett.* **2004**, *45*, 2747−2749.

(56) Poole, L. B.; Klomsiri, C.; Knaggs, S. A.; Furdui, C. M.; Nelson, K. J.; Thomas, M. J.; Fetrow, J. S.; Daniel, L. W.; King, S. B. Fluorescent and Affinity-Based Tools To Detect Cysteine Sulfenic Acid Formation in Proteins. *Bioconjugate Chem.* **2007**, *18*, 2004−2017.

(57) Wellendorph, P.; Jaroszewski, J. W.; Hansen, S. H.; Franzyk, H. A sequential high-yielding large-scale solution-method for synthesis of philanthotoxin analogues. *Eur. J. Med. Chem.* **2003**, *38*, 117−22.

(58) Lovric, M.; Scholz, F. Modeling cyclic voltammograms of simultaneous electron and ion transfer reactions at a conic film three-phase electrode. *J. Electroanal. Chem.* **2003**, *540*, 89−96.

(59) Lovric, M.; Komorsky-Lovric, S. Distribution of three ions in the thin film experiment. *Electrochem. Commun.* **2003**, *5*, 637−643.

(60) Rieke, P. C.; Armstrong, N. R. Light-assisted, aqueous redox reactions at chlorogallium phthalocyanine thin-film photoconductors: dependence of the photopotential on the formal potential of the redox couple and evidence for photoassisted hydrogen evolution. *J. Am. Chem. Soc.* **1984**, *106*, 47−50.

(61) Korzeniewski, C.; Callewaert, D. M. An enzyme-release assay for natural cytotoxicity. *J. Immunol. Methods* **1983**, *64*, 313−20.

(62) Decker, T.; Lohmann-Matthes, M. L. A quick and simple method for the quantitation of lactate dehydrogenase release in measurements of cellular cytotoxicity and tumor necrosis factor (TNF) activity. *J. Immunol. Methods* **1988**, *115*, 61−9.

(63) Alley, M. C.; Scudiero, D. A.; Monks, A.; Hursey, M. L.; Czerwinski, M. J.; Fine, D. L.; Abbott, B. J.; Mayo, J. G.; Shoemaker, R. H.; Boyd, M. R. Feasibility of drug screening with panels of human tumor cell lines using a microculture tetrazolium assay. *Cancer Res.* **1988**, *48*, 589−601.

(64) Knight, J. C.; Wuest, M.; Saad, F. A.; Wang, M.; Chapman, D. W.; Jans, H.-S.; Lapi, S. E.; Kariuki, B. M.; Amoroso, A. J.; Wuest, F. Synthesis, characterisation and evaluation of a novel copper-64 complex with selective uptake in EMT-6 cells under hypoxic conditions. *Dalton Trans.* **2013**, *42*, 12005−12014.

(65) Blower, P. J. A nuclear chocolate box: the periodic table of nuclear medicine. *Dalton Trans.* **2015**, *44*, 4819−4844.

(66) Fodero-Tavoletti, M. T.; Villemagne, V. L.; Paterson, B. M.; White, A. R.; Li, Q.-X.; Camakaris, J.; O'Keefe, G.; Cappai, R.; Barnham, K. J.; Donnelly, P. S. Bis (thiosemicarbazonato) Cu-64 Complexes for Positron Emission Tomography Imaging of Alzheimer's Disease. *J. Alzheimer's Dis.* **2010**, *20*, 49−55.

(67) Torres, J. B.; Andreozzi, E. M.; Dunn, J. T.; Siddique, M.; Szanda, I.; Howlett, D. R.; Sunassee, K.; Blower, P. J. PET imaging of copper trafficking in a mouse model of Alzheimer disease. *J. Nucl. Med.* **2016**, *57*, 109−114.

(68) Lewis, J. S.; McCarthy, D. W.; McCarthy, T. J.; Fujibayashi, Y.; Welch, M. J. Evaluation of ^{64}Cu-ATSM in vitro and in vivo in a hypoxic tumor model. *J. Nucl. Med.* **1999**, *40*, 177−183.

(69) Hueting, R.; Kersemans, V.; Cornelissen, B.; Tredwell, M.; Hussien, K.; Christlieb, M.; Gee, A. D.; Passchier, J.; Smart, S. C.; Dilworth, J. R.; Gouverneur, V.; Muschel, R. J. A comparison of the behavior of ^{64}Cu-acetate and ^{64}Cu-ATSM in vitro and in vivo. *J. Nucl. Med.* **2014**, *55*, 128−134.

(70) Solomon, B.; Binns, D.; Roselt, P.; Weibe, L. I.; McArthur, G. A.; Cullinane, C.; Hicks, R. J. Modulation of intratumoral hypoxia by the epidermal growth factor receptor inhibitor gefitinib detected using small animal PET imaging. *Mol. Cancer Ther.* **2005**, *4*, 1417−1422.

(71) Donnelly, P. S.; Xiao, Z.; Wedd, A. G. Copper and Alzheimer's disease. *Curr. Opin. Chem. Biol.* **2007**, *11*, 128−133.

(72) Xiao, Z.; Donnelly, P. S.; Zimmermann, M.; Wedd, A. G. Transfer of Copper between Bis(thiosemicarbazone) Ligands and Intracellular Copper-Binding Proteins. Insights into Mechanisms of Copper Uptake and Hypoxia Selectivity. *Inorg. Chem.* **2008**, *47*, 4338−4347.

(73) Rubino, J. T.; Franz, K. J. Coordination chemistry of copper proteins: How nature handles a toxic cargo for essential function. *J. Inorg. Biochem.* **2012**, *107*, 129−143.

(74) Tateishi, K.; Tateishi, U.; Sato, M.; Yamanaka, S.; Kanno, H.; Murata, H.; Inoue, T.; Kawahara, N. Application of ^{62}Cu-diacetyl-bis (N4-methylthiosemicarbazone) PET imaging to predict highly malignant tumor grades and hypoxia-inducible factor-1α expression in patients with glioma. *AJNR. Am. J. Neuroradiol.* **2013**, *34*, 92−9.

(75) Yoshii, Y.; Matsumoto, H.; Yoshimoto, M.; Zhang, M.-R.; Oe, Y.; Jin, Z.-H.; Tsuji, A. B.; Yoshinaga, K.; Fujibayashi, Y.; Higashi, T.; Kurihara, H.; Narita, Y. Multiple Administrations of ^{64}Cu-ATSM as a Novel Therapeutic Option for Glioblastoma: a Translational Study Using Mice with Xenografts. *Transl. Oncol.* **2018**, *11*, 24−30.

(76) Hickey, J. L.; Lim, S. C.; Hayne, D. J.; Paterson, B. M.; White, J. M.; Villemagne, V. L.; Roselt, P.; Binns, D.; Cullinane, C.; Jeffery, C. M.; Price, R. I.; Barnham, K. J.; Donnelly, P. S. Diagnostic Imaging Agents for Alzheimer's Disease: Copper Radiopharmaceuticals that Target Aβ Plaques. *J. Am. Chem. Soc.* **2013**, *135*, 16120−16132.

(77) Caragounis, A.; Du, T.; Filiz, G.; Laughton, K. M.; Volitakis, I.; Sharples, R. A.; Cherny, R. A.; Masters, C. L.; Drew, S. C.; Hill, A. F.; Li, Q.-X.; Crouch, P. J.; Barnham, K. J.; White, A. R. Differential modulation of Alzheimer's disease amyloid-β peptide accumulation by diverse classes of metal ligands. *Biochem. J.* **2007**, *407*, 435−450.

(78) Dorow, D. S.; Cullinane, C.; Conus, N.; Roselt, P.; Binns, D.; McCarthy, T. J.; McArthur, G. A.; Hicks, R. J. Multi-tracer small animal PET imaging of the tumor response to the novel pan-Erb-B inhibitor CI-1033. *Eur. J. Nucl. Med. Mol. Imaging* **2006**, *33*, 441−52.